



New Technologies for Benthic Habitat Mapping

Literature study

HANS KAUTSKY, MICHAEL TULLDAHL, OVE STEINVALL,
NIKLAS STRÖMBECK, SOFIA WIKSTRÖM

FOI är en huvudsakligen uppdragsfinansierad myndighet under Försvarsdepartementet. Kärnverksamheten är forskning, metod- och teknikutveckling till nytta för försvar och säkerhet. Organisationen har cirka 1000 anställda varav ungefär 800 är forskare. Detta gör organisationen till Sveriges största forskningsinstitut. FOI ger kunderna tillgång till ledande expertis inom ett stort antal tillämpningsområden såsom säkerhetspolitiska studier och analyser inom försvar och säkerhet, bedömning av olika typer av hot, system för ledning och hantering av kriser, skydd mot och hantering av farliga ämnen, IT-säkerhet och nya sensorers möjligheter.



FOI
Totalförsvarets forskningsinstitut
Informationssystem
Box 1165
581 11 Linköping

Tel: 013-37 80 00
Fax: 013-37 81 00

www.foi.se

FOI-R--3013--SE Teknisk Rapport
ISSN 1650-1942 June 2010

Informationssystem

Hans Kautsky, Michael Tulldahl, Ove Steinvall,
Niklas Strömbeck, Sofia Wikström

New Technologies for Benthic Habitat Mapping

Literature study

Titel	Nya teknologier för kartering av bottenhabitat
Title	New Technologies for Benthic Habitat Mapping
Rapportnr/Report no	FOI-R--3013--SE
Rapporttyp Report Type	Teknisk Rapport Technical Report
Sidor/Pages	56 p
Månad/Month	June
Utgivningsår/Year	2010
ISSN	ISSN 1650-1942
Kund/Customer	Naturvårdsverket
Projektnr/Project no	B53008
Godkänd av/Approved by	Johan Allgurén

FOI, Totalförsvarets Forskningsinstitut

Avdelningen för Informationssystem

Box 1165

581 11 Linköping

FOI, Swedish Defence Research Agency

Information Systems

P.O 1165

SE 581 11 Linköping

Sammanfattning

Det finns en stor efterfrågan på kartor av undervattensmiljöer som underlag för exploatering och bevarande av kustområden. Denna rapport är en litteraturstudie av befintliga och framtida tekniker och metoder för att framställa kartor av biotoper under vatten som är baserade på faktiska observationer. Vi strävar efter att hitta metoder för generering av kartor på samma sätt som sker med flygfotografering, den vanliga informationskällan för många landbaserade kartor. Fokus i rapporten är kartläggning av bottenmiljöer med laser och andra optiska tekniker från luftburna plattformar. Andra tekniker (ekolod), metoder (fältobservationer, spatiell modellering) och plattformar (satelliter, yt- och undervattensplattformar) berörs kortfattat. Rapporten innehåller en kort sammanfattning av de metoder som används idag för kartering av grunda växt- och djursamhällen.

Vår slutsats är att flera nya tekniker är av intresse för kartering av bottenhabitat. För befintliga och nya sensorer, förutses att metoder kommer att utvecklas genom bättre och mer automatiserade algoritmer för sammanslagning av data. Detta omfattar både sammanslagning av data från olika sensorer (t.ex. laser och passiva bilder) och fjärranalysdata med data från fältmätningar. För de grundaste områdena, ned till ett par meter under vattenytan är flygburna multi- eller hyperspektrala kameror av stort intresse för kartläggning, eftersom de erbjuder ökade möjligheter att skilja mellan naturtyperna. Flygburen laserteknik för djupmätning kan idag betraktas som operativ teknik. Med utveckling av sensor och algoritmer kan flygburen laser bli en viktig metod för kartläggning av grunda bottenhabitat. Framtida lasersystem med högre effektivitet tillsammans med känsliga mottagare kan utveckla systemen att omfatta flera våglängdskanaler, fluorescens, Raman och andra spektrala metoder för att öka prestanda för klassificering och kartläggning. Utveckling av autonoma plattformar kan minska kostnaderna för insamling av data. Små flygburna plattformar kan redan idag vara användbara för kartering av bottenhabitat i grunda områden.

Denna rapport är en del (akvatiskt arbetspaketet 3, WPA3) av arbetet inom EMMA-projektet (Environmental Mapping and Monitoring with laser And digital images) som finansieras av svenska Naturvårdsverket. Fokus i EMMA-projektet är att använda data från operativa flygburna system tillsammans med fältobservationer från t ex undervattensvideo, men i WPA3 studeras även framtida teknik av intresse för utveckling på längre sikt. Det slutliga målet är att uppnå snabba, noggranna och automatiska metoder som täcker stora områden och beskriver ekosystemens tillstånd i grunda vatten längs den svenska kusten.

Nyckelord: Kartering av bottenhabitat, vegetation, klassificering, laser, lidar, fluorescens, multispektral, hyperspektral

Summary

There is a demand from the authorities to have good maps of the coastal environment for their exploitation and preservation of the coastal areas. The subject of this report is a literature study of the state-of-the-art and possible future methods for producing maps of the biota under water that are based on actual observations. We aim to find methods for generation of actual maps of the biota the same way as is done with aerial photography, the evident base for most land based maps. The focus of the report is benthic (sea bed) habitat mapping with laser and other optical techniques from aerial platforms. Other mapping techniques (sonar), methods (field observations, spatial modelling) and survey platforms (satellites, underwater and surface platforms) are briefly discussed. The report includes a brief summary of the methods used up to today to map shallow plant and animal communities.

We conclude that several new technologies are of interest for benthic habitat mapping. For existing and new sensors, we foresee that the methodology will be developed by better and more automated algorithms for data exploration and for fusing different data sets together. For the first few metres below the sea surface, airborne and spaceborne, passive multi- or hyperspectral imaging systems are of great interest for mapping. Airborne laser techniques for collection of depth can be considered as operational. With sensor and algorithm development the airborne depth sounding laser is a highly interesting method for mapping of shallow underwater habitats. Future laser systems with higher efficiency together with high-sensitivity receivers may enable laser systems which include multiple-wavelength channels, fluorescence, and other spectral techniques to increase classification and mapping performance. Development of platforms with autonomous operation can reduce cost of operation and limit manpower involvement. Small aerial platforms may already today be useful for low-cost benthic habitat mapping in the most shallow areas.

This report is a part (Aquatic Work Package 3, WPA3) of the work within the EMMA project (Environmental Mapping and Monitoring with laser And digital images) financed by the Swedish Environmental Protection Agency, SEPA. The focus in the EMMA project is on using remote sensing data from operational systems on airborne platforms, but in WPA3 we also consider future technologies of interest in a long-term view. The ultimate goal is to obtain quick, accurate and automatic methods that cover large areas and show the actual state of the shallow-water ecosystems along the Swedish coast.

Keywords: Benthic habitat mapping, vegetation, classification, laser, lidar, fluorescence, multispectral, hyperspectral

Contents

1	Introduction	7
2	Requirements for Habitat Mapping	9
3	Current Operational Methods - Brief Overview	11
3.1	Satellite Data.....	12
3.2	Aerial Photography	13
3.3	Echo-Sounding, Side-Scan Sonar	13
3.4	Underwater Video	13
3.5	Other Sampling Techniques	14
4	Recent Studies of Methods for Habitat Mapping	15
4.1	Satellite Imagery	15
4.2	Hyperspectral Aerial Imagery.....	18
4.3	Airborne Laser Scanning	19
4.4	Other Methods for Habitat Mapping.....	20
5	Emerging Technologies and Trends	24
5.1	Fusion of Lidar Data and Hyper- or Multispectral Imaging	24
5.2	Lidar System Development.....	26
5.3	Topographic Complexity from Lidar Data	27
5.4	Ultrafast Cameras	27
5.5	Active Spectral Imaging	28
5.6	Gated Viewing.....	29
5.7	Streak Tube Imaging Lidar.....	29
5.8	Laser Line Scanner.....	30
5.9	Polarisation Imaging	30
5.10	Laser Induced Fluorescence.....	31
5.10.1	Example of Systems and Studies of Fluorescence	31
5.11	Laser Induced Breakdown Spectroscopy	35
5.12	Raman Techniques.....	35
5.13	Conclusion and Comments for Imaging Systems.....	36
6	Platforms	37

6.1	Autonomous Underwater Vehicles (AUV) and Gliders	37
6.2	Unmanned Surface Vessels (USV)	37
6.3	Unmanned Aerial Vehicles (UAV)	38
7	Performance Estimates for Airborne Scanning Lidar Concepts	42
8	Conclusions	49
	References	51

1 Introduction

The subject of this report is a literature study of the state-of-the-art and possible future methods for producing maps of the biota under water that are based on actual observations. We aim to find methods for generation of actual maps of the biota the same way as is done with aerial photography, the evident base for most land based maps. The rule today under water is to draw maps of the biota which are derived from statistical models predicting the probability of occurrence of the plant and animal communities, and where actual observations only are a minor fraction of the area illustrated. To achieve our aim, we have two problems, the possibility to be able to observe the occurrence of the plant and animal communities every single metre of the sea floor below the water column and to be able to interpret the signals obtained. We need one or a combination of techniques to see through the water column and to learn how to interpret and allocate the signals from our devices to the plant and animal communities of interest.

In this report a brief summary is presented of the methods used up to today to obtain broad scale pictures of the shallow plant and animal communities. There are several ongoing or just finished programmes dealing with the problematic of sea floor mapping (e.g. the reports from the EU-interregional programmes of MESH (<http://www.searchmesh.net/>) and BALANCE for current methods (<http://balance-eu.org/publications/index.html>, <http://balance-eu.org/xpdf/balance-interim-report-no-30.pdf>, http://balance-eu.org/xpdf/balance-interim-report-no-27_draft.pdf). The goal has been to find operative methods to produce accurate maps of the shallow communities along our coast. The ongoing EU SeaMap (2009-2010) continues the approach of drawing maps from scattered information. Also within the project INFOMAR (<http://www.infomar.ie>) coastal biotopes for shallow areas were mapped, where echo sounders (multibeam) and airborne LIDAR were used for the bathymetry (Coggan *et al.* 2007). In Norway similar projects, but with a distinct emphasis on deeper communities is ongoing within the project MAREANO, which to date have produced detailed maps of the northern parts of the Norwegian continental shelf (<http://www.mareano.no/>). Similarly, the program MopoDeco tries to develop methods using models and simulations to map the sea floor. Within that project the main drawback pointed out is the lack of relevant data to make adequate maps with appropriate quality and resolution, i.e. the problem of drawing maps of area coverage from little real data (actual observations). The Baltic Sea Action Plan hosted by HELCOM gathers countries around the Baltic Sea, and a compilation of programmes performed in the Baltic Sea region was done within their project BIO (http://www.helcom.fi/projects/Archive/en_GB/BIO/).

There is a demand from the authorities to have good maps of the coastal environment for their exploitation and preservation of the coastal areas. During the last years several ambitious programmes to survey potential Natura 2000 areas was conducted by the coastal counties in Sweden. Thus, our general knowledge of what species can be expected in shallow enclosed bays, pristine archipelago areas and offshore reefs has improved dramatically. The surveys were performed with various methods having in common a visual approach (snorkeling, SCUBA diving, video transects). These methods provide a good description of the habitat and species composition in the investigated spots, but due to the small spatial cover they only had the possibility to actually describe a fraction of the area of interest.

The Swedish EPA (SEPA) was commissioned to lead the work to compile biological data of the habitat types of the Swedish seafloor and to produce maps with the different, relevant GIS layers (Regeringsuppdrag 25) (Naturvårdsverket 2009). The report presents several ongoing or recently finished projects with the aim to map the sea floor. Due to the lack of full coverage data, the maps of species and habitats presented in the recent report were mainly based on spatial modelling that predict the occurrence of species. Although spatial modelling is a well accepted method for providing full-coverage maps, it is important to remember that they are based on field data that cover only a fraction of the

mapped area. This means that the maps show a statistical prediction of species distributions and they can never be expected to give a perfect description of the actual distribution. The report had the intention to further encourage efforts to find new, comprehensive methods to map the habitats and species distribution on the seafloor. The authors point out the need of good maps to be used as background information for the increased exploitation of the seas. Another example of ongoing programmes in Sweden deals with the mapping of the off shore reefs for potential marine wind mill parks (SEPA Regeringsuppdrag 27), where the approach is similar to "Regeringsuppdrag 25". Another report presents further analyses of the biological data collected during the inventory of Swedish offshore banks carried out during 2003-2005 (Naturvårdsverket 2008).

This report is a part (Aquatic Work Package 3, WPA3) of the work within the EMMA project (Environmental Mapping and Monitoring with laser And digital images) financed by SEPA. The aim of the EMMA-project is to find ways to produce maps of the biota under water that are based on actual observations. There is a demand for improvement of the current methods. The focus of the EMMA project is on remote sensing data from *operational* systems on airborne platforms, but in the project WPA3 we also include new approaches which will be considered for experimental studies in field and in laboratory. The ultimate goal is to develop quick, accurate and automatic methods that cover large areas and give us an actual state of the shallow-water ecosystems along the Swedish coast.

2 Requirements for Habitat Mapping

During historical times there has always been a demand for good maps on land for orientation and for planning of military field campaigns and later on also for the building of the modern infrastructure such as railways. Today, on land it is evident that maps always serve as the prime background information for the detailed planning of the society. The choice of resolution is from a few dm to the whole country, based on aerial photography and or satellite images.

In the marine environment, maps with accurate information of the depth were needed for navigation, e.g. along the trades. For military purposes, more accurate maps have been produced the last 100 years, but they also have a variation in resolution and accuracy. From the start, most depths were obtained by handheld leads and positioning by the eye. To draw more accurate navigation charts or maps of the bottom topography the development of eco-sounding and later side-scan sonar and multibeam sonar in combination with exact positioning (recently satellite GPS) have improved the charts dramatically. Still, they do not have a complete and detailed coverage as any topographical map of the land may have, mostly because the instrument platforms (ships) cannot go everywhere.

In the shallowest areas down to a few metres depth, the lack of accurate depth data with high resolution is most pronounced. In the shallow depths the echo-sounder, side-scan and multibeam methods usually are not operative due to the backscatter being too close or only an extremely narrow footprint on the bottom (which increases with depth) is obtained. The lack of accurate depth charts in the marine environment has been addressed by the authorities the later years and the EMMA-project is one example of how solutions for this problem are searched for.

The planning authorities have a demand for good maps. On land these maps are present, and there is an ongoing process within many fields to improve the maps, involving numerous people all over the world. The contents of the maps may at any time be checked by either simple field observations or detailed studies of the original data (e.g. aerial photography, satellite etc). Also here, there is a demand to improve the accuracy by making the interpretation of the signals from remote sensors more automatic and accurate without involving the interpretation by the human eye. This demand is addressed within the terrestrial part of the EMMA-project.

In contrast to the terrestrial system, there is a general lack of maps of seabed habitats, although there have been several attempts to improve our knowledge of the sea bottom along our coasts. Within the SAKU and BALANCE programmes, maps were drawn for single species and communities along the Nordic coasts. What all these maps had in common was that they were based on models. While maps of modelled distributions may be useful for planning, there is a risk that they might be interpreted as showing the actual conditions of the sea floor. Authorities are well acquainted with land maps and know their accuracy. A map reflects what is written in the subtext. The marine map however, is usually based on statistical models which predict what might be expected at a given site. This is perhaps not so far from how the land maps are produced, but there we can track and verify every m^2 if necessary. In the marine environment we know how it looks like along e.g. a 100 m long diver transect line ($600-1000 m^2$) or in a 0.5 m by 0.5 m square observed by a snorkler or video drop camera. The total cover of actual observations in field, which serve as base for the marine maps produced today is only a minor fraction of the whole area illustrated. If lucky, $600-4000 m^2$ (divers transects, depending of the length and how many transects are performed in the area) to perhaps $10-100 m^2$ (drop video or snorkel) are the base for the model. The occurrence of the species in the remaining, typically several km^2 of the area illustrated in the map are estimated by the models. The models usually take into account the depth and wave exposure and sometimes the inclination and the type of substrate to make their predictions. Their performance is highly dependent on the accuracy and resolution of these environmental data. Typically, good

bathymetric maps are lacking. What the models usually cannot take into account is the patchiness and the mosaic distribution of the seabed communities.

It is important to understand that mapping with statistical modelling gives only a statistical probability of what might be on a given site within the marine environment. Therefore, we urgently need data that covers the area of interest which in turn can be interpreted accurately. For this there is a need of a twofold approach within the marine environment. First we need to develop methods that give us a total area cover as obtained on land by, e.g. airborne photography and/or satellite. The data must be of high resolution to be able to solve the second approach where, we need to develop methods (learn) how to interpret signals from remotes that they adequately describe the ecosystem. We need to learn how to distinguish between the vegetation and the seabed substratum, and even better, to distinguish between species or groups of species. When this is achieved, we will be able to deliver maps to the authorities that accurately describe the ecosystem and that can be used for planning and decisions within the society.

Airoidi and Beck stress the importance of mapping the biotopes along the coast of the European coast to estimate the habitat loss (Airoidi and Beck 2007). In a similar way accurate maps may serve as a tool for monitoring of shallow water biotopes and see temporal changes of, e.g. the NATURA 2000 areas and other BSPAs.

3 Current Operational Methods - Brief Overview

In this section we briefly describe current methods used for benthic habitat mapping. Recently, within the ICES-TIMES series, Kautsky reviewed the methods used within the phytobenthic communities (Kautsky 2009). Depending on the question asked, the collection of data is a matter of scale. The collection of data goes from remote observations to direct observations, and sample collection and analysis. All methods have advantages and disadvantages and may be appropriate within a given context. There is a trade-off between the large-scale data and the detailed descriptions, as between cost and benefit. Some methods are good compromises and are applicable in various concepts within the dynamics of the phytobenthic plant and animal communities.

If we consider the spatial scale, there is a trade-off between the area covered and the information gained (usually also coupled to the time spent in field and laboratory), see Figure 1. Satellite data cover the largest areas but usually with little information and low resolution (pixel sizes of 50 m x 50 m and in special cases down to about 1 m x 1 m). Usually, all time is spent interpreting the data signal and no time in field. Aerial photography can only cover limited regions, usually one image-frame typically covers 500 m x 500 m. However, the resolution is much higher than the satellite image and objects down to metre-size or less can be observed. A new technique is using airborne laser techniques for the bathymetry down to approximately 15 m depth in the Baltic Sea region (dependent on the turbidity of the water). It can thus be used to produce charts of high resolution which is necessary for efficient planning of surveys and modelling of results. The next step in laser technology will be to separate different types of vegetation and substrate and thus be able to map vegetation zones and their depth extension. Ship borne registration tools usually are not limited by depth (e.g. echo sounder and sonar) and may operate within the depth zone where vegetation can be found (the phytobenthic zone) without problems (video hanger and ROV). There is an increase in information content and decrease in area covered when going from video hanger or remotely operated vehicles (ROV) to diver observations. The non-visual methods require longer time in lab for the interpretation of data signals. The highest resolution and information is gained by quantitative sampling, either by frame pictures or destructive sampling. Destructive sampling is by far the most costly method as it requires tedious sorting in lab. In suitably shallow waters, also snorkelling and e.g. an Aquascope can be used with success. The intertidal area may need no equipment. Quantitative samples may be obtained by area observations (fixed or thought squares) and/or pictures from given distances or by destructive sampling of standard areas adapted to the studied objects.

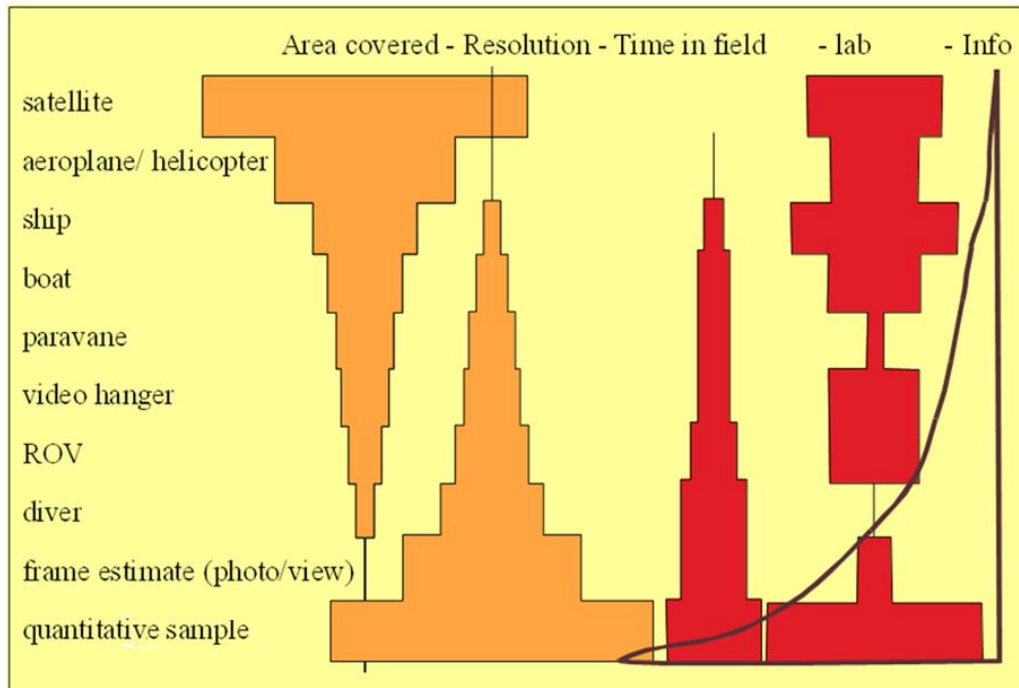


Figure 1. A schematic view of different approaches in field comparing the proportion between area covered, spatial resolution, time in field and processing data (lab) and detail obtained.

3.1 Satellite Data

Satellite Multispectral Imaging has been used to map the land and sea for military, commercial, and environmental purposes for many years. If the proper wavelengths are selected, multispectral images can be used to detect bathymetric features and benthic habitats. This technique is especially useful for mapping of shallow shelf areas where deposition, erosion, and growth of coral reefs can change bottom topography over the period of a few years (Sabins 1997).

The greatest limitations to the collection of multispectral images are atmospheric conditions (cloud cover), water turbidity, water depth, sun glint from the sea surface, and reflectance of sediment and vegetation on the seafloor. In addition, despite the satellite's ability to cover an extremely large area (several km), the resulting image resolution is low (sometimes on the order of several hundred meters).

Today, optical satellite data is mostly used to monitor pelagic production. The technique may have a potential in phytobenthic communities but development of methods (signal - interpretation) is needed. Also, routines have to be developed to handle the immense amounts of data with reasonably high resolution (1x1m to 10x10m grids). Another major drawback is that the obtained images cannot see deeper down than a few meters into the water column (in temperate waters). Exceptions may be in clear waters, where satellite data have been used to map coral reef distribution, and seagrass meadows. Also, an atmospheric disturbance (clouds etc) limits the number of usable images to a few per year in many regions. Data from satellites can show the water turbidity, major outflows from land and thus provide with essential data for the interpretation of results from phytobenthic studies especially when large scale models are used (see e.g. Kratzer and Tett 2009).

3.2 Aerial Photography

Relatively large areas can be covered by aerial photography. The images often allow observations down to about 3 m depth in Nordic waters, but in clear water areas (e.g. Mediterranean, tropical areas) it can be used to map vast areas down to several meters depth. The resolution is in general high (about 0.1 m) at least close to the surface under ideal conditions. However, the method is weather dependent (limited by clouds and/or strong winds). Also, the solar elevation angle will affect the results by reflections from the water surface and sea surface waves can be a limiting factor for the image quality. The images need ground proofing for the interpretation of the observed structures.

Aerial photography has successfully been applied in mapping reed belts (Finland), shallow bays, shallow e.g. *Zostera*- and *Fucus*- communities (Swedish West coast, locally on the east coast), in mapping *Posidonia* meadows, the intertidal Watt area Northern Germany and in mapping coral reef extension etc.

A relatively new, potentially interesting method is under development where laser depth data is used for correction of the aerial imagery. The method is further described in Sections 4 and 5 of this report.

3.3 Echo-Sounding, Side-Scan Sonar

The echo sounding and side scan sonar techniques can cover large areas, with a relatively high resolution (about 0.1 m). The techniques have no depth limit and give well to excellent depth information (multibeam). Especially the sonar technique gives good estimates of the substrate type, and they can detect plant cover. The drawback is that all data signals need interpretation and calibration through ground proofing. The signals are dependent on the layers in the water column and may generate different results of due to change in water temperature and/or salinity etc. There is a the need for improved interpretation of the signals and optimal choice of methods (e.g. which frequency to chose for a given purpose).

The methods have successfully been used in producing marine geological maps (side-scan sonar) in the mapping of e.g. *Posidonia* meadows in the Mediterranean and seagrass beds in the USA. There are ongoing projects to improve the signal interpretation using echo sounding (e.g. NIVA-Simrad, etc.).

3.4 Underwater Video

There are a wide variety of deployment techniques for obtaining underwater video data, including boat-deployed drop, towed, or remotely operated vehicle (ROV) systems, as well as diver hand-held systems. Although the value of the underwater video data is very dependent upon water clarity, the video data can provide valuable insight into the qualitative water column and seafloor conditions.

When using a video hanger the data obtained are visual and no signal interpretation is needed. The camera can be towed over a relative large distance and thus cover the depth range of the photic zone within one video session or km-long, horizontal distance. The resolution is high (about 0.01 m) especially when the camera is towed slowly (<1 knot). The data from the video profile can be documented and interpreted along transects lines along a known depth gradient. An alternative for large scale habitat mapping, as used along the entire coast of Finland, is central or random points within a grid which are video-documented using a drop camera. A random proportion of squares with in the grid are visited and documented. The grid size may be standardized, e.g. 1x1 km, or be of different size, depending on the expected heterogeneity of the area. The observations are done just around the point where the camera is dropped (1-2 m²). The results are presented as large scale maps of species distribution.

Each video picture should always be accompanied by the exact positioning (GPS) and depth information. Also, temperature should be included when e.g. observing fish. The equipment can be inexpensive (well functioning systems for around € 1000 are found on the web). The documentation on tapes gives excellent opportunity to go back to the material for verification or for viewing it from new perspectives. However, the instability of the picture caused by the video hanger camera movement and wave induced ship movement makes it sometimes hard to exactly see what is on the image and some ground proofing is needed. The method has successfully been used in e.g. habitat mapping of offshore shallow reefs in the Baltic Sea. It may serve as a survey tool for finding suitable stations for diving transects in e.g. the start up phase of monitoring programmes. The major drawback is the unstable image depending on the ship movement in combination with the usually narrow field-of-view (FOV) of the camera lens. These problems may to a part be solved by technical improvement of the equipment, but turbidity may still be a limiting factor for using wide-FOV systems. A vertical down-looking camera gives a limited view of the surrounding and therefore it is recommended that another camera is added which has a more horizontal view.

3.5 Other Sampling Techniques

Sediment-profile imaging (SPI) gives vertical cross-section photographs (in situ profiles) of the upper 15 to 20 cm of the seafloor surface. Employing a specially designed camera and frame, SPI is a discrete sampling technique used for rapid collection, interpretation, and mapping of data on physical and biological seafloor characteristics. As opposed to all of the other optical techniques (both boat and aircraft deployed), SPI is not negatively impacted by poor water clarity. Rapid computer-aided analysis of each sediment profile image yields a suite of standard measured parameters, including sediment grain size major mode, camera prism penetration depth (an indirect measure of sediment bearing capacity/density), small-scale surface boundary roughness, depth of the apparent redox potential discontinuity (RPD, a measure of sediment aeration), infaunal community, and Organism-Sediment Index (OSI, a summary parameter reflecting overall benthic habitat quality) (Rhoads and Germano 1982).

Plan-view photography is another discrete sampling technique that employs a frame-mounted downward looking camera to obtain plan-view photographs of a small patch (typically 2m²) of the seafloor surface. The plan-view images provide an undisturbed view of the seafloor surface and are useful for indicating sediment composition and surface biological activity.

Beside the above mentioned sensing technologies, a number of physical sampling techniques exist which give a detailed analysis of selected parts of the water and sea bottom.

4 Recent Studies of Methods for Habitat Mapping

This section describes some of the recent work and development in habitat mapping using satellite imagery, aerial hyperspectral imagery, and airborne laser scanning. In the last subsection, work with combinations and comparisons of these sensor data with other data sources is described.

4.1 Satellite Imagery

For assessing morphologically complex underwater environments, satellite sensors with high spatial resolution is needed. Here, we therefore focus on so-called VHR sensors (Very High Resolution 0.5-5 m). As a general trade-off today, a good spatial resolution means that spectral resolution is reduced. While present operational Earth Observation satellites can have up to 15 narrow spectral bands (MERIS) in the visible and near infrared domain, VHR sensors generally have four wide bands of about 50-100 nm width: blue, green, red and near infrared. This is good enough for most commercial applications where focus is on good image acquisitions and positioning, while it is less useful for assessing aquatic underwater environments, as in-water spectral features usually are quite wide. Thus, using VHR sensors in this context means that we need to work with spectrally reduced data. Below follows a brief overview of which sensors that can be used today and in the near future.

Civil use of VHR sensors kicked off with the successful launch of IKONOS in 1999. Before that, VHR data had mainly been accessible for military intelligence. IKONOS has a spatial resolution of 0.82 m panchromatic (black and white acquisition) and 3.2 m multispectral (in the four spectral bands described above). It has a return time of 3 to 5 days (144 days for true-nadir) and 11-bit resolution. Since its launch it has formed the basis of the company GeoEye. The company's second VHR sensor, GeoEye-1 was launched in 2008. It has a spatial resolution of 0.41 m panchromatic and 1.65 m multispectral. However, only U.S. Government customers and specifically designated customers have access to this resolution while commercial customers receive imagery at the highest resolution allowed by U.S. regulations, currently 0.5 m. The sensor is 11-bit and has a return time of about three days. In the near future (2011-2012) the company will also launch GeoEye-2 with even better specifications and a spatial resolution of 0.25 m panchromatic.

Public use of VHR data was even more triggered by Digital Globe's series of VHR sensor. Supply of data started in 2001 with QuickBird-2. However, QuickBird-2 was the company's third VHR sensor, preceded by EarlyBird and QuickBird-1, both failing to reach orbit. QuickBird-2, commonly referred to as just QuickBird, has since then formed the basis of popular commercial services like e.g. Google Earth. It has a spatial resolution of 0.61 m panchromatic and 2.44 m multispectral, is 11-bit and has a return time of about three days in Scandinavia. Digital Globe's next interesting sensor, WorldView-2, is planned to be launched on October 8 2009. In contrast to all other VHR sensors described here, it will not only have a high resolution panchromatic band, but also eight multispectral bands: the four common bands red, green, blue and near-infrared and four new bands violet-indigo (called coastal), yellow, red edge and near-infrared (called NIR2 and partly overlapping the other near-infrared band). Panchromatic spectral resolution will be 0.46 m and multispectral resolution 1.8 m. The sensor is 11-bit and return time will be around four days.

Another series of VHR sensors that can be of interest for the future is the Pléiades (1 and 2) from the French Space board CNES. CNES has also support from the National Swedish Space Agency which can allow for good access to images. The Pléiades are planned for 2010-2011 and they will be very similar to QuickBird in their specifications.

Malthus and Karpouzli investigated the use of satellite data (IKONOS multispectral, 4 m resolution) in clear waters to evaluate its suitability for discriminating typical shallow water habitat types (Malthus and Karpouzli 2003). They applied corrections for water depth with depth digitised from the hydrographic map and interpolated the values to produce a bathymetric model. A preliminary supervised maximum likelihood classification was performed on the depth-corrected image using training areas of known surface types defined from biological surveys conducted in the field. For a number of surfaces (e.g. seagrass and intertidal areas) several training zones were required. Three sand types were differentiated: exposed beach sand, submersed medium-coarse sand and submersed fine-medium-grained sand. Rock surfaces were differentiated as exposed algal-covered and bedrock surfaces, submersed bedrock and rock ridges. Submersed plant coverages were separated into algal and seagrass types. Areas of seagrass and submersed algae showed some confusion as a result of having similar spectral reflectance properties. Areas of fine and medium-coarse sand are probably well delineated, but overclassified in regions of patchy seagrass distribution. The water column correction was successful for most of the area of interest with only the deeper waters (approximately > 8.5 m) showing signs of noise as a result of the model working against the limit of light penetration. For the accuracy assessment of the classification 58 independent ground-truthed stations were used which were not included in the training of the supervised classification. Sand categories dominated the ground-truthed dataset as the survey was essentially a random one and sand is the dominating substrate in the area. The overall classification accuracy was 60.3%. Some patches of seagrass were confused with fine sand, probably because the patches of seagrass were both sparse and smaller than the image pixel resolution of 4 m. Many other habitats were also confused with sand categories although this may also be due to imprecision in positioning of the actual ground-truth stations and the patchy nature of the habitats in the region.

Wennberg *et al.* (Wennberg *et al.* 2007) evaluated SPOT-5 satellite imagery as a tool to characterise shallow habitats in the Baltic Sea. Four sensor channels was used for the analysis: green channel XS1 (0.50-0.59 μm), red channel XS2 (0.61-0.68 μm), near infrared channel XS3 (0.78-0.89 μm), and shortwave infrared XS4 (1.58 to 1.75 μm). The pixel size was 10 m * 10 m except for XS4 where the pixel size was 20 m * 20 m. Three areas with different coastal types and water characteristics were studied. The northernmost site was the area around Holmöarna in the southern Bothnian Bay, the middle area, Uppland, was a scene which covers large parts of the coast and archipelagos in Uppsala county in the southern Bothnian Sea and the southernmost area covers the northern part of Stockholm archipelago in the northern Baltic proper. Reference data of submerged and emergent vegetation, water depth and Secchi depth was collated from field surveys. The data were used for calibration in the satellite image analyses as well as for validation of the results. Different classifications of *submerged* vegetation were tested, including different classes of cover and colour of the vegetation. The species were classified into red, green and brown species, but analyses of the spectral information as well as artificial neural network (ANN) analyses showed that it was not possible to separate between vegetation of different colour with satisfying result. In the final ANN analyses, vegetation species cover for 10 m * 10 m or 10 m * 1 m was estimated in classes 0-4. Total cover (%) per sample area were then recalculated as the sum of 2.5% (cover class 1), 15% (cover class 2), 40% (cover class 3) and 75% (cover class 4). Analyses were performed to distinguish between areas with high and low vegetation cover and each sample point was classified into different vegetation cover categories: 0-20, 20-80 and >80% vegetation cover. Including depth as a predictor did not increase the accuracy of the interpretations, while including Secchi depth, which could only be done for Uppland, seemed to be central for achieving adequate classification. Thus only in the Uppland scene the classification met the required accuracy level. The overall accuracy was 51.9% in the Uppland scene. Neither in this scene the overall accuracy was very high, but in most cases incorrectly classified pixels were classified to the adjacent class. The vegetation classification for Stockholm was not useful, as almost no vegetation was identified. For Holmöarna the maximum vegetation class was captured to some extent, but not the other classes. The analysis of the

Holmöarna scene may have been negatively affected by large difference in data capturing date, as the satellite scene was from mid June while the reference data was from August. The reported results for classification of *emergent* vegetation were more accurate. An overall accuracy of 70 - 75 % was obtained for the classes "Open water", "Water, non-open surface", "Reed on land", "Reed in water", and "Land".

Kutser (Kutser, Vahtmae, and Metsamaa 2006) used satellite measurements for the three common Baltic Sea species *Fucus vesiculosus*, *Furcellaria lumbricalis* and *Cladophora glomerata* in the attempt to make maps along the Estonian coast (a project within BALANCE). Although the species could be depicted in special cases (when growing on contrasting sandy substrates, the method could not be used to determine their depth distribution. They stated that “configuration of MERIS spectral bands allows the recognition of red, green and brown macroalgae based on their spectral signatures provided the algal belts are wider than MERIS spatial resolution.” Kutser *et al.* (Kutser, Vahtmae, and Martin 2006) used the method described above in clear waters (Australia) obtaining better results, indicating the problem with the Baltic Sea water colouring and transparency.

By measurement and analysis of the whole reflectance spectra from a water body, it is in some cases possible to estimate both water depth, bottom type and optical properties of the water column. The work by Maritorena *et al* can serve as an introduction to this field as they refer to several early studies (Maritorena *et al.* 1994). The authors themselves studied how reflectance of shallow water is influenced by water depth and bottom reflectance. They provided data of reflectance of several types of bottoms from French Polynesia (Fig. 1). Other early, and since then well referred work outlining this, was made by Lee and co-workers in the nineties (Lee *et al.* 1994; Lee *et al.* 1998, 1999). Essential for their approach was to use a well functioning and parameterized semi-analytical optical model in order to objectively describe the relevant optical processes in the water. In their models, e.g. measured and modelled data of the spectral absorption and scattering coefficients, fluorescence and reflectance of different bottom types (bottom Albedo) were used. In the environment studied, these bottoms included relatively high-reflecting examples of sand, silt or clay. By inversion of the models, the authors could assess water depth with good accuracy. However, as input data, spectral reflectance from ship-borne hyperspectral instruments were used. No efforts were then made using operational remote sensing data.

The field become more explored during late nineties and early two thousands when the process commonly referred to as “coral bleaching” become generally acknowledged. Shortly, coral bleaching is the trivial term for whitening of corals due to stress-induced expulsion or death of symbiotic algae, or due to the loss of pigmentation within the algae. Coral bleaching can be induced by e.g. changes in water temperature, increased solar irradiance notably in the UV-domain or changes in water chemistry. Due to the often very large size of coral reefs, remote sensing was proposed as a potential monitoring tool. In 2003, the highly acknowledged scientific journal *Limnology & Oceanography* (ASLO 2003) published a special issue called *Light In Shallow Waters*. This special issue summarized a lot of the work from many research groups and several collections of bottom reflectance can be found therein, predominantly from tropical or sub-tropical waters. Kutser and co-workers (Kutser *et al.* 2003) used an approach similar to Lee and co-workers where they simulated the possibilities of using different air-borne and satellite sensors for monitoring coral reef health based on separation and identification of different bottom types. A spectral library of coral reef benthic communities was collected from the Great Barrier Reef including live coral, dead coral, soft coral, sand, brown algae, green algae, red algae and cyanobacteria. Their basic conclusion was that hyperspectral sensors allow for good identification of different bottoms, while sensors with broader and fewer bands provide less possibility. In another study Stumpf and co-workers (Stumpf *et al.* 2003) showed early success in using the VHR sensor IKONOS to assess water depth in clear waters with shifting bottom reflectance.

Even though there are plenty of data of bottom reflectance around for tropical or subtropical waters, the situation is different for the Baltic. Kutser and co-workers (Kutser, Vahtmäe *et al.* 2006) presented a library of algae and different substrates from Estonian coastal waters of the Baltic and compared them to earlier work. The library was focusing on the brown alga *Fucus vesiculosus* (Bladder wrack, Sw. blåstång), the green alga *Cladophora glomerata* (Blanketweed, Sw. grönslick) and the red alga *Furcellaria lumbricalis* (Black carrageen, Sw. kräkel/gaffeltång) as these species were selected as indicator species for the Baltic by HELCOM. One conclusion from their measurements was that Baltic species show the same spectral features connected to their pigments as do algae of the same groups from different parts of the world. In a later publication (Vahtmäe and Kutser 2007), the library was used to estimate bottom vegetation from satellite remote sensing. Two different satellite sensors were used: 1) QuickBird with four wide spectral bands and a spatial resolution of 2.4 m and 2): Hyperion with a spatial resolution of 30 m and around 200 bands of 10 nm width. It was concluded that QuickBird rendered the best results, mainly due to its much better spatial resolution. However, it was also stated that its few spectral bands was a limiting factor. As a way to improve the estimations, they referred to the concept of contextual editing (Mumby *et al.* 1998), i.e. inferring information of known species distribution with e.g. depth.

4.2 Hyperspectral Aerial Imagery

Airborne Hyperspectral Imaging is a technology that has recently been used to classify benthic habitats in coastal zones. Hyperspectral sensors can collect several hundred spectral bands of data at a high spatial resolution usually between 400 and 900 nm. In order to match the spectral data to those of known reflection or absorption spectra careful calibration has to be made taking into account water surface, altitude, atmospheric and water transmission properties. For typical flight altitudes the spatial resolution range between 1 and 25 meters. The number of bands has to be adapted to the species of concern to maximize available signal to noise ratios. The integration time has to be long enough to collect sufficient photons during the measurement. The resulting product is a high-resolution, geo-referenced image, which can be imported into a GIS.

The technique has been successfully used to classify tropical benthic habitats including coral reefs, seagrass, macroalgae (fleshy and turf), unconsolidated sediments, uncolonized hard-bottom areas, and encrusting algae. Where aerial photography may fail, airborne hyperspectral imaging can be useful for submerged aquatic vegetation (SAV) mapping. It can provide potential detail on species composition in addition to biomass estimates. Hyperspectral Imaging also has its limitations. It has low availability and may not be cost-effective. Also, because of its ability to collect several hundred bands of data at high resolution, somewhat advanced software is needed to process and analyze these data. In addition, it is primarily useful in shallow, non-turbid waters, as are most electro-optical techniques. Recent work has included combining lidar and HSI.

Andrefouet *et al.* (Andrefouet *et al.* 2004) used compact airborne spectrometer imager (CASI) hyperspectral measurements of the tropical marine flora of 2 South Pacific Ocean coral reefs and could discriminate between broad patches of reef, algae and sand. They concluded: Comparison of the wavelengths identified from in situ and airborne measurements allowed definition of a subset of common wavelengths that were robust to changes in spatial scale and still provided excellent discrimination and classification accuracy between the ecological groups. These results suggest that continuous spectral signatures acquired in situ at the centimetre scale can be used to select key discrete wavelengths for remote-sensing observations of communities at the meter scale despite the spatial heterogeneity in benthic cover and the resulting spectral mixing.

Therriault *et al.* (Therriault *et al.* 2006) used a range of spectra (airborne hyperspectral sensor (CASI) to collect 19 channels of ocean colour data at 1 m² spatial resolution (spanning from 391 nm to 904 nm) in an effort to accurately map benthic communities

(*Codium fragile*) over 7 km² of seabed to a water depth of 6 m (south coast of Nova Scotia Canada). Pure patches of the invasive algae, kelp, and sand were clearly distinguishable at scales of 1m² to 1,000m².

Mishra *et al.* (Mishra *et al.* 2007) presented a coral reef application using data from a Hyperspectral Airborne Imaging Spectroradiometer for Applications (AISA). The hyperspectral imagery was used in band ratio algorithms to derive water depth and water column optical properties (e.g., absorption and backscattering coefficients) followed by a water column correction technique for generation of substrate reflectance on a per-pixel basis. The approach needs clear waters as in these coral reef areas. The authors state that airborne hyperspectral sensors seem to be appropriate for overcoming the lack of both high spectral and spatial resolution of satellite sensors.

Phinn *et al.* evaluated seagrass classification from aerial images (Phinn *et al.* 2008), where airborne hyperspectral image data were acquired from a CASI-2 sensor using a pixel size of 4 m. Also, two types of multispectral satellite image data were used: Quickbird 2 and Landsat 5 TM. The work included field data validation, but did not incorporate corrections of image data for depth and turbidity. The study was performed in clear water not representative of the Swedish coastal water types. Classification was made on depths down to 3 m, and thus image pixels from deeper depths were rejected. Their results demonstrated that mapping of seagrass cover, species and biomass to high accuracy levels (>80%) was not possible across all image types. For each parameter mapped, airborne hyperspectral data produced the highest overall accuracies (46%), followed by Quickbird 2 and then Landsat 5 TM.

4.3 Airborne Laser Scanning

Airborne laser scanning, also called lidar (light detection and ranging), for characterisation of marine environments is gaining an increased interest. An example is the work by Populus *et al.* (Populus *et al.* 2004), where airborne *topographic* laser scanning and photogrammetry was studied for habitat mapping applications in the intertidal zone. Méléder *et al.* (Méléder *et al.* 2007) examined the ability of airborne bathymetric laser scanning to characterise seabed substratum types. A methodology using slopes and isobaths allowed the distinguishment of three substrata: rocky, soft and a transition substratum.

Vegetation classification from laser bathymetry waveform data in less clear coastal waters was studied by Tulldahl *et al.* (Tulldahl *et al.* 2007; Tulldahl *et al.* 2008), where an overall classification accuracy of greater than 80% (Tulldahl *et al.* 2008) was obtained compared to field data for eelgrass, sand and dark algae. The main goal of the work was to examine the feasibility to classify bottom types with characteristic properties in vegetation height and reflectance. Thus, experimental data was examined from a site with low reflectance algae, high reflectance sand and eelgrass having high reflectance in green and significant height above the sea floor. The study showed reasonable agreement between lidar classification and reference data taken from underwater video. The video data was taken about 10 months after the lidar survey. Consequently, a complete evaluation of the classification accuracy was not achievable due to possible changes in the sea floor properties and vegetation between the measurements.

In another work Collin *et al.* (Collin *et al.* 2008) used waveform data backscattered from the bottom and concluded that bathymetric lidar backscatters can significantly differentiate between the four characterized habitats. Representative samples of the four habitats included: (1) boulder with Asteroidea (sea stars), (2) fine sand with dejecta of polychaetes, (3) *Laminaria* sp. on boulder, and (4) echinoids on cobble.

Brock *et al.* used lidar techniques to investigate the rugosity (topographic complexity) of coral reefs off Florida to estimate the occurrence of fish (Brock *et al.* 2006; Kuffner *et al.* 2007). In another work, the biodiversity was studied in relation to rugosity, where the rugosity was estimated from underwater video imagery (Shumway *et al.* 2007).

The potential of laser scanning for assessing river bathymetry has been evaluated by Hilldale and Raff (Hilldale and Raff 2007) aiming at applications such as flow hydraulics, flood routing, sediment transport, aquatic habitat, and monitoring of geomorphology. The mapping of pool, riffle and glide features were possible with the survey quality, while smaller objects on the order of a large cobble were on the limit to be resolved.

The drawback of the lidar system to detect the sea floor for rough and varying substrates was discussed by Pe'Eri *et al.* 2007.

Wedding *et al.* (Wedding *et al.* 2008) reported successful results using lidar for the determination of the sea floor rugosity, which has an implication of the fish habitats on coral reefs. They described an application to see habitat complexity and to derive estimates of fish biodiversity.

The authors Nayegandhi *et al.* (Nayegandhi *et al.* 2009) used methods to filter away the response of the canopy to achieve the bare ground data. "Results presented in the study confirm the cross-environment capability of a green-wavelength, waveform-resolving lidar system, making it an ideal tool for mapping coastal environments". Makes it interesting when the filtered data are put back again as an indication of vegetation cover.

Costa *et al.* (Costa *et al.* 2009) compared lidar with multibeam echo sounding MBES for providing benthic habitat (biotope) maps of coral reef ecosystems. They found that "lidar cost 6.6% less than MBES and required 40 fewer hours to map the same study area. MBES provided more detail about the seafloor by fully ensonifying high-relief features, by differentiating between fine and coarse sediments and by collecting data with higher spatial resolutions.

In addition, there are several relevant examples, descriptions and references of habitat mapping with airborne lidar, found under the following home pages:

<http://ngom.usgs.gov/dsp/pubs/ofr/index.html> and

<http://ngom.usgs.gov/dsp/pubs/manuscripts/index.html>.

4.4 Other Methods for Habitat Mapping

In an overview of eelgrass mapping methods (Precision-Identification 2002), several methods and case studies were reviewed. The methods included aerial photo, side scan sonar, and underwater video. A case study in Willapa Bay, Washington State described a benthic mapping project using aerial photography. The accuracy assessment incorporated an approach of segmenting the SAV (submerged aquatic vegetation) data by bathymetry to allow potential habitat to be sampled as well as mapped areas. The baseline study was completed in 1995; and the investigators felt that the subsequent annual studies relying on aerial photographs, was effective for detecting changes in the aerial coverage of each species eelgrass (*Zostera marina* and *Z. japonica*) and *Spartina alterniflora*, an aggressive non-native species. A relevant study for Swedish waters was the environmental monitoring program related to the construction of Öresundsbron between Denmark and Sweden. Some areas were field-verified by diving along transects. Biomass samples were used to develop signatures based on texture from the photographs. The biomass in each area was estimated based on the signature. Additional samples were collected to determine the accuracy of the interpolation. The turbidity of the water was low when the air photographs were taken and it was possible to detect eelgrass down to, and in some cases beyond the 6 m bathymetric gradient. Air photo interpretation proved sensitive enough to detect annual variations, both increases and decreases, each year between 1996 and 1998. The accuracy of the analysis was lowest near the depth limit of eelgrass where reflection from the vegetation was lowest, due to the reduced coverage and biomass of the plants. The Massachusetts

Department of Environmental Protection (DEP) Wetlands Conservancy Program (WCP) has developed a project to map the seagrasses, specifically *Zostera marina* and *Ruppia maritima* along the entire Massachusetts' coastline. The project used air photo interpretation (NOAA standards) and extensive fieldwork to map the coastal seagrasses. The mapping process involved the following steps: 1. Acquisition of Aerial Photography 2. Photo interpretation of seagrass beds 3. Fieldwork to confirm Photo-interpreted features 4. Compilation to Digital Base Map 5. Independent Accuracy Assessment Procedure. The digital base map was produced and an accuracy assessment conducted. The 'assessment was based on random points generated with the polygon boundaries'. A real time differential GPS was used to navigate to each point in the field. The assessment indicated that about 85 % of the beds had been correctly mapped. The investigators declared that the maps should be considered conservative, due to limitations associated with the air photo interpretation. The following factors were believed to contribute to the underestimation; 1. the aerial photograph might have been captured when atmospheric and hydrospheric conditions were less than ideal, 2. the experience of the photointerpreter, 3. nature of the subject area (dark underwater substrate), and, 4. the quality and amount of surface level field data.

Sabol *et al.* compared acoustic and aerial photography methods for mapping of submerged aquatic vegetation (SAV) (Sabol *et al.* 2008). They concluded that their acoustic technique detected considerably more SAV than does the standard aerial photographic technique. True-color near-vertical photography was taken with a handheld camera from 200 m and 1000 m elevation. The acoustic system, Submersed Aquatic Vegetation Early Warning System (SAVEWS) consisted of a digital echo sounder and global positioning system. Most of the contiguous areas of acoustically detected, high coverage, tall (>0.5 m) SAV that were missed by aerial photography occurred near the delineated eelgrass polygons but in deeper waters. The investigators assume that this was caused by depth limitations to the photo interpretation capability or possibly some horizontal positional error associated with the delineated polygons. The question of acoustically distinguishing between eelgrass and other species was not addressed in the study.

The SAKU-project, financed by the Swedish EPA, mainly worked with models and GIS applications with the goal to have seamless maps of the biota along the entire Swedish coast. Within the SAKU project the importance of good environmental data (layers) of, e.g. the type of substrate and the bathymetry was emphasised. The lack of good geological maps relevant for the biota and the lack of detailed bathymetric maps for the country were seen as a major problem. Within the SAKU project a model for the calculation of the wave exposure was developed (Isaeus 2004). The wave exposure model with a 25x25 m grid improved the models used in SAKU and oncoming work.

The interregional programme BALANCE continued to have the goal of presenting maps along the Scandinavian marine coasts. A thorough description of methods involved for the field observations was presented. The maps drawn were based on models, where more or less good background data of the depth, type of substrate (geology), wave exposure were the included driving forces. The total area of actual field observations was only a small fraction of what the maps presented. The quality of the maps were shown to be strongly linked to the quality and quantity of hard data (field observations) and environmental information (depth, type of substrate, salinity etc).

One of the most comprehensive approaches to map the coastal area was performed within the MESH programme <http://www.searchmesh.net/>. The Mesh programme (Development of a framework for Mapping European Seabed Habitats) is a European Union INTERREG IIB funded marine habitat mapping programme developing international standards and protocols for seabed mapping (<http://www.searchmesh.net/>). The aim was to compile existing habitat maps and to harmonize them to the EUNIS classification system. In their report they give a good literature review and overview of the methods that can be used for mapping of the seafloor (Coggan *et al.* 2007).

Tuell *et al.* (Tuell and Park 2004; Tuell *et al.* 2005) have demonstrated the potential to produce estimates of green laser reflectance and optical properties of the water column by analyzing laser waveforms; this in turn provides for the fusion of laser, multi- and hyper-spectral digital imaging for classification of sea floor vegetation. They used the SHOALS laser system and the CASI hyperspectral sensor. The SHOALS system typically collects data on a 4m x 4m grid from a flying height of 400m. The data was interpolated from individual data points into 5 m pixels. The image processing strategy was based on the SHOALS sampling resolution and implied that the higher CASI spatial resolution was sacrificed. This decision was made for computational convenience. Furthermore, the investigators state that high resolution passive images are more significantly perturbed by water surface and require rigorous approaches to position the pixels on the seafloor. In this regard, spatial averaging to larger 5 m pixels was beneficial for producing images of the seafloor. The collected CASI data had rectangular pixels with a nominal resolution of 0.5 m across track and 1.0 m along track. From these 5m pixels were generated to match the resolution of the SHOALS images. The radiance values in the final images were computed as the average value of radiance for all image pixels within the 5m pixel. The CASI bandset consisted of 32 contiguous spectral bands from 426 nm to 972 nm; each band has a FWHM bandwidth of 17 nm. The work by Tuell *et al.* is an example where *depth* and *water turbidity* are used for correction of aerial images. Their algorithms were tested in clear waters and were not subjected to any validation against bottom reflectance field data or to the classification of sea floor features or vegetation.

In the waters of Hawaii lidar (SHOALS) was used for the bathymetry (Gibbs *et al.* 2006). In combination with aerial photographs (colour) and underwater video and still photography, maps were drawn using models based on substrate structure, the substrate % cover of the major biota components and geographic zone (geomorphology of reefs). They presented nice maps but concluded that more scuba divers transects for were needed for proofing and that airborne infrared or hyperspectral imagery could be used to isolate spectrally unique bio-indicators to improve the maps.

In the offshore reef surveys off the Swedish coast a traditional investigation of the geology was performed using side-scan sonar. The vegetation was surveyed with hanging video and/or ROV. A combination of depth, type of substrate and the knowledge of biota was used in a model to draw maps of the habitats (Naturvårdsverket 2008).

Hochberg and Atkinson (Hochberg and Atkinson 2008) used the optical absorbance to determine the productivity along a range of spatial scales on a coral reef Hawaii. They used QuickBird satellite imagery and SHOALS lidar data. The results indicated that the method might be developable.

Chust *et al.* 2008, used lidar in combination with multispectral photography in the intertidal environments along the Spanish Atlantic coast. The lidar provided detailed bathymetry which was used in data models to estimate the probability of different habitat mainly taking into account the slope and aspect of the sea floor. By using different spectral filtering and correlations with the multispectral imagery data they could increase the accuracy of the method detecting characteristic habitats.

Foster and Jesus (Foster and Jesus 2006) used portable, low-cost hyperspectral radiometers in the intertidal zone to measure different algal reflectance and calibrated their results with airborne and satellite data. They found their method promising.

Thorhaug *et al.* (Thorhaug *et al.* 2007) made comparisons of spectral reflectance of different plants in Atlantic waters. They concluded that spectral reflectance data appear potentially useful for remote sensing of shallow habitats, and may additionally be used to monitor their health.

Foster and Jesus (Foster *et al.* 2006) presented the use of three single beam acoustic seafloor discrimination systems (QTCView, Echoplus, Biosonics) in shallow ocean water for the evaluation of algae seasonality, biomass and coral reef benthos density and distribution. Accuracy comparisons were performed against classified IKONOS and

Landsat imagery as well as interpreted lidar bathymetry maps. The comparisons showed optical imagery to have superior discriminatory ability in shallow water only. The study indicates that results from optical and acoustic surveys have some degree of commonality. Therefore, there is a potential to produce maps outlining tropical benthos from optical remote-sensing in shallow water and acoustic methods in adjacent deeper areas beyond optical resolution with the limitation that acoustic maps will resolve fewer habitat classes and have lower accuracy.

5 Emerging Technologies and Trends

The above given description of different sensing and sampling techniques can be foreseen to be developed further with new technology, new platforms and new system concepts and way of performing measurement campaigns. In this section we describe some of these emerging technologies, platforms and methods.

On *technology*, we will concentrate on laser sensing which will be further developed from line scanning and depth sounding lidars to include fluorescence, Raman and other spectral techniques to increase classification and concentration estimate of different objects and molecules. Laser imaging will be used taking advantage of high resolution 3 D imaging as well as active multi- or hyperspectral capabilities. Laser sensing will also be combined with passive EO sensing and with other sensor like acoustics.

The methodology will be developed by better and more automated algorithms for data exploration and for fusing different data sets together. Routines for combining different sensors together into practical sensor suites will be improved as well as how to combine remote sensing with in situ sampling more efficiently.

5.1 Fusion of Lidar Data and Hyper- or Multispectral Imaging

Terrain, sea and bottom mapping may be improved by combining passive hyperspectral imaging (HSI) data with lidar data. The benefits are particularly useful when working in the littoral zone where it is possible to use bathymetric lidar to facilitate estimation of water column attenuation coefficients and seafloor reflectance from passive spectral data. The estimates of attenuation reveal information about the optical properties of the water, and active and passive seafloor reflectance can be used cooperatively to achieve seafloor classification.

We will give some examples of recent work in this area. Optech (Tuell *et al.* 2005) recently described collected SHOALS-1000 (lidar) and Casi data (HSI) simultaneously over the South Florida Testing Facility (SFTC) in Dania Beach, Fl. to support development of REA (Rapid Environmental Assessment) data fusion algorithms.

Figure 2 (a) shows the SHOALS ρ_{532} image of a 3 km x 5 km area of the seafloor lying immediately south of the entrance channel to Port Everglades, Fl. Here, the bottom morphology consists of a series of reefs paralleling the coast which are separated by regions of sand, seagrass, and mixed vegetation. The prominent feature running vertically along the right side of Figure 25 is the third reef seaward of the beach. This reef is a spur and groove formation lying in depths as deep as 30m. The narrow, horizontal feature in the lower third of Figure 25 is a sewer outfall pipe. The terminus of the pipe lies at a depth of about 28 m, and its outfall plume can be clearly identified as an area of lower reflectance. The dark, rectangular feature near the centre of the image is a borrow pit in a sand ridge between the second and third reefs.

Figure 2 (b) shows the SHOALS $(a_{532}(\text{absorption}) + b_{532}(\text{backscatter}))$ image of the same area. This image has been formed by estimating attenuation for each pulse. Here, the outfall plume can be clearly identified as an area of higher attenuation, and the triangular area in the upper left corner is an abrupt area of attenuation change. The speckled appearance of the image indicates the noisy nature of the estimation process. For this reason, we typically smooth the $(a_{532} + b_{532})$ images with a 25x25 element boxcar filter before using them in the inversion of the passive RTE s.

Figure 2 (c) shows the Casi ρ_{534} image. This image is a mosaic of 11 separate Casi flight lines acquired with the aircraft trajectory aligned to the solar azimuth. In the process, the lines were radiometrically balanced.

Together, Figure 2 (a) and Figure 2 (c) represent active and passive reflectance from datasets collected simultaneously. In shallow waters (depths less than 20m), the images look highly similar. However, in deeper waters the contrast and resolution in the passive image degrades significantly when compared to the SHOALS image.

A procedure combining lidar and HSI data generated seafloor reflectance estimates for 11 channels of data from 426 to 611nm. Using these data, a false colour image of the seafloor using the 602nm, 534nm, and 450nm images can be obtained (Figure 3 (a)). Figure 3 (b) shows classification of the coral reef pixels.

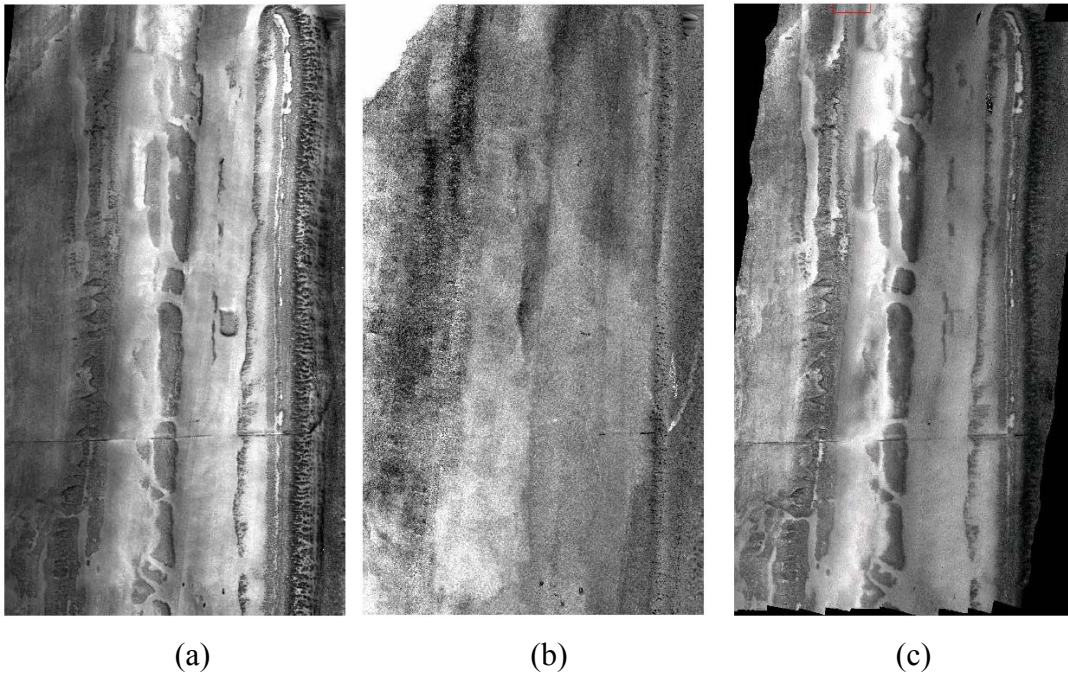


Figure 2. (a) SHOALS ρ 532 image, (b) SHOALS (a532+bb532) image, (c) Casi ρ 534 image. From Optech (Tuell *et al.* 2005).

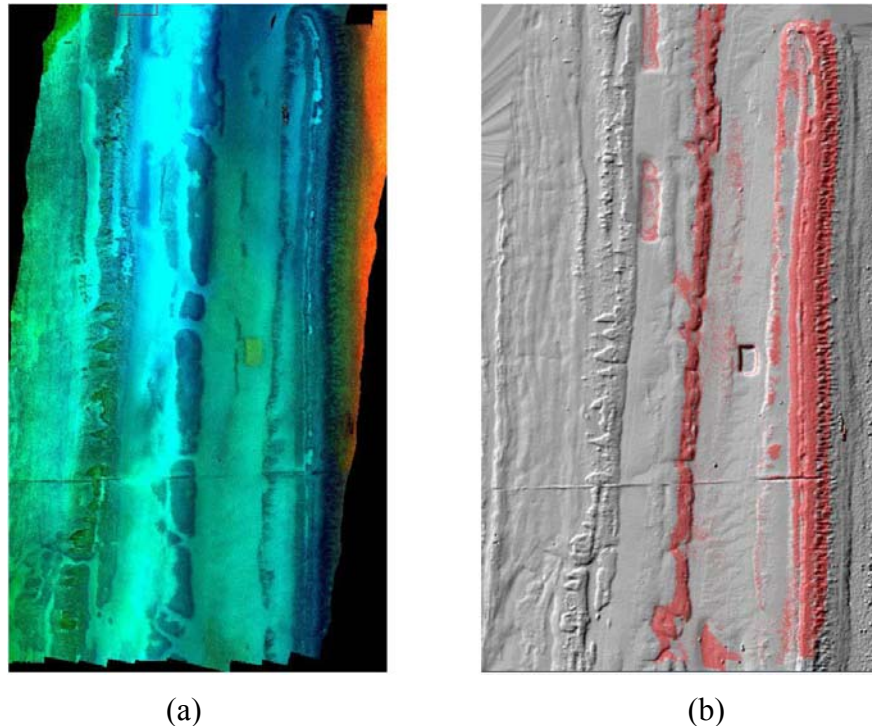


Figure 3. (a) False color image (602, 534, 450 nm), (b) Classification of coral reef pixels (in red). From Optech (Tuell *et al.* 2005).

Kopilevich *et al.* (Kopilevich *et al.* 2005; Feygels *et al.* 2005) propose a concept for estimation of ocean optical properties with a multiple field-of-view bathymetric lidar using Optechs SHOALS system. The SHOALS design uses two receivers for depth measurement: a shallow-water, APD receiver with an 18 mrad FOV; and a deep-water PMT receiver with a 40 mrad FOV. They simultaneously record the optical power returned from a single pulse of the laser, and consequently provide the desired measurements. They present an algorithm for the estimation of inherent optical properties (IOPs) in the upper ocean layer based on “multiple-forward-single-backscattering” model of the returned power, and an analytical solution to the radiative transfer equation (RTE) for finite sounding beam propagation in the small-angle-scattering approximation. The IOP’s estimates are the backscattering coefficient, the beam attenuation coefficient, the single-scattering albedo, and the VSF asymmetry coefficient, obtained by fitting simulated waveforms to actual data measured by the two receivers. They also present an approach for improvement in estimates of bottom reflectance which compensates for pulse stretching induced by angle of incidence effects.

5.2 Lidar System Development

The future development for airborne oceanographic lidar systems will include higher resolution and high area coverage rate using very sensitive detector arrays (single photon sensitivity), miniaturization (smaller lasers, power equipment etc..) and multisensor use combining laser scanning with Hyperspectral imaging. By this combination the data will not only be improved from each sensor but the combination will lead to new capabilities as indicated above. In a longer perspective we see the development for active spectral sensing (see subsection 5.5).

Single photon counting lidars have been demonstrated by Sigma Space Cooperation (<http://www.sigmaspace.com/>) in the US for NASA and other customers. The demonstrated an equivalent sampling rate of 2.2 million soundings per second. One photon

per range measurement gives very efficient systems. The technique is proven for both night and day operation through gating of the receiver and applying post-detection filters to extract the signal from the background during daytime operation. The single photon sensitivity combined with multistep detection and timing allows to see through obscurations such as haze, thin clouds and turbid waters. The high sensitivity also allows sounding from space with modest telescope sizes (< 1m) and with a laser power of a few watts.

5.3 Topographic Complexity from Lidar Data

In a work by Tuell, an ONR-financed programme, *Countermine Lidar UAV-based System (CLUBS)* (<http://www.onr.navy.mil/Science-Technology/Departments/Code-32/All-Programs/Atmosphere-Research-322/Environmental-Optics/Annual-Report-FY07.aspx>), examples are given on the combination of lidar and passive EO data for bottom classification and for extraction of the water parameters in the water column. This work also includes generation of *rugosity metrics* (calculated from *SHOALS depth*) and combined these features into a lidar feature space.

As noted in subsection 4.4, Brock *et al* (Brock *et al.* 2006) examined the ability to discriminate cluster zones of massive stony coral colonies on northern Florida reef tract patch reefs based on their topographic complexity (rugosity) using data from an experimental lidar called EAARL. They correlated the lidar data with underwater photography.

Tulldahl and Wikström (Tulldahl and Wikström 2010) performed separability tests of bottom types using a multivariate classification method. Based on evaluation of a large number of waveform-derived classification variables a preliminary set of four variables. With the preliminary set of variables a total classification accuracy of about 70% was obtained between the four bottom types Sand, Low Vegetation, High Vegetation and Boulders. This illustrates that when combined with depth-derived variables (in this case slope and depth standard deviation), the waveform variables have the potential to substantially improve classification accuracy of substrates and vegetation. It was found that a combination of several variables can be appropriate for separation of different bottom types and vegetation. For example, the bottom roughness can be captured either by a waveform variable such as the bottom echo pulse rise time, or the standard deviation of depths in the vicinity of a lidar sounding. These two variables both indicate roughness but on slightly different scales.

5.4 Ultrafast Cameras

Ultrafast, light-sensitive video cameras are needed for observing high-speed events such as shockwaves, communication between living cells, neural activity, laser surgery and elements of blood analysis. To catch such elusive moments, a camera must be able to capture millions or billions of images continuously with a very high frame rate. Conventional cameras are simply not up to the task. This technique may have interesting capabilities to capture and identify species using both the time and spectral domain and is called “serial time-encoded amplified microscopy” (STEAM).

Now, researchers at the UCLA have developed a novel, continuously running camera that captures images roughly a thousand times faster than any existing conventional camera. The capture rate of images were observed at some 6 million frames per second.

In a paper by Goda *et al.* in the April 30 issue of Nature (Goda *et al.* 2009) an entirely new approach is described for imaging that does not require a traditional CCD (charge-coupled device) or CMOS (complementary metal-oxide semiconductor) video camera. This is due in part to a technological limitation - it takes time to read out the data from sensor arrays. Also there is the fundamental trade-off between sensitivity and frame rate; at high frame

rates, fewer photons are collected during each frame – a predicament that affects virtually all optical imaging systems. Goda *et.al.* describe a new type of imaging which maps a two-dimensional (2D) image into a serial time-domain data stream and simultaneously amplifies the image in the optical domain. It captures an entire 2D image using a single-pixel photodetector. Achieving a net image amplification of 25 dB (a factor of 316), it overcomes the trade-off between sensitivity and frame rate – without having to resort to cooling and high-intensity illumination. Continuous real-time imaging at a record frame speed of 163 ns (a frame rate of 6.1 MHz) and a shutter speed of 440 ps is achieved, and demonstrates its use in imaging ultrafast microfluidic flow in real time.

5.5 Active Spectral Imaging

The area of active spectral imaging will be partly covered in the fluorescence imaging section below. We will here report some other interesting technologies which have relevance for underwater problems.

Recent development of broadband lasers and advanced imaging 3 D receivers has led to new opportunities for advanced spectral and polarization imaging with high range resolution. The broad emission in supercontinuum white light lasers eliminates the problems with passive hyperspectral or multispectral imaging namely the conversion of the measured radiance to reflectance information. This conversion can be difficult due to for passive sensors, due to the changing geometry between the sun, target and sensor which can affect the reflectance, and also introduce shadows in the scene. The inherent reflectance spectrum is one of the key measures for material classification. The active imaging can also give night capability including colour information.

Using short pulsed lasers and detectors with a fast time response a 3D imaging capability is obtained allowing improved penetration capabilities through vegetation, camouflage, water, atmospheric haze and obscurants. Discrimination capabilities can be further enhanced through the addition of polarization and fluorescence measurements.

A group at MIT have been exploring active spectral sensing (Nischan *et al.* 2003) . They have conducted a series of laboratory and field tests to demonstrate the utility of combining active illumination with hyperspectral imaging for the detection of concealed targets in natural terrain. The active illuminator, developed at MIT Lincoln Laboratory, was a novel microlaser-pumped fiber Raman source that provides high-brightness, subnanosecond-pulse-length output spanning the visible through near-infrared spectral range. The hyperspectral-imaging system was comprised of a compact, grating-based spectrometer that uses a gateable, intensified CCD array as the detector element. The illuminator and hyperspectral imaging system were mounted on a tripod and scanned in azimuth to build an image scene of up to several hundred spectral bands. The system was deployed under a variety of environmental conditions, including night-time illumination, and on a variety of target scenes, including exposed and concealed plastic and metallic mine-like targets. Targets were detected and identified on the basis of spectral reflectance, fluorescence signatures, degree of polarization, and range-to-target information (via range gating). Imaging performance was evaluated by detection of two green plastic objects in green vegetation as a function of spectral resolution. The target objects included pieces of green and black plastic, an optical taggant (a brightly coloured plastic disk impregnated with a fluorescing dye), a metal wire, and a shell casing. All of the objects were partially concealed by grass and weeds in a natural setting that also included soil and rocks. The fusion of the fluorescence, polarization, and white-light images allowed detection and discrimination of all of the targets in the scene. Other examples of active hyperspectral imaging were made by BAE in the UK (Bishop *et al.* 2007).

5.6 Gated Viewing

Range gated systems can be used to extend the imaging range compared to conventional underwater video. A good example of a state of the art system is described by Fournier (Fournier *et al.* 1993). Tulldahl *et al.* (Tulldahl *et al.* 2006) reported on trials showing that images can be acquired at significantly longer distances with the gated camera, compared to a conventional video camera. The distance where a target can be detected was increased by a factor of 2. For images suitable for object identification, the range improvement factor is typically 1.5. Examples of image processing of the range-gated images were tested, which increased the image quality significantly. Gated viewing has been used for applications in air (Steinvall *et al.* 2007) and comparable underwater systems have been tested since the seventies. A system with mm range resolution is presented by Busck (Busck 2005). The author at former FOFT in Denmark has recently demonstrated high resolution imaging with sub mm accuracy for the identification of sea mines and other applications like personal identification. The main components of the laser radar system are a green pulsed laser and a fast gating intensified CCD camera. The laser radar system innovation is a combination of the short laser pulses (0.5 ns), the high laser pulse repetition rate (32.4 kHz), the fast gating camera (0.2 ns gate width) and short camera delay steps (0.01-0.1 ns).

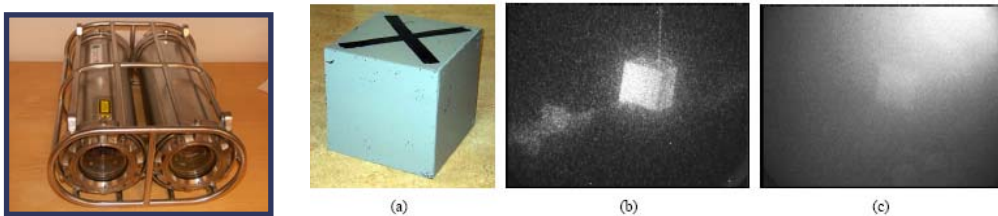


Figure 4. Left a range gated system using a green laser. Right show the target (a) and the images in gated (b) and non gated modes (c). Images FOI (Tulldahl *et al.* 2006).

Range gated systems can also be used through the air-sea interface. The Magic Lantern System by Kaman Aerospace (USA) was used successfully in the Gulf war to detect the presence of subsurface suspended mines (Ulich *et al.* 1997). Another system, by Churnside *et al.* have been investigating surveys of epipelagic fish (Churnside and Wilson 2001; Churnside and Wilson 2004; Churnside *et al.* 1997).

5.7 Streak Tube Imaging Lidar

The STIL technique (Jaffe *et al.* 2001) is an advancement of a gated camera developed by Areté Associates. The system has been developed for military applications and is now in service in the US Navy. As a lidar system, STIL measures the time of flight. However, a new feature is its capability to measure the amplitude of the backscattered signal as well. This data can be processed to form both a contrast image and a range image, in order to provide a full 3-D representation of the underwater scene.

According to the web page of Areté Associates they have two Streak Tube Imaging LIDAR (STIL) systems currently in production for the United States Navy. The first is the Airborne Mine Detection System (ALMDS). This helicopter-deployed active electro-optical sensor performs wide-area mine detection and classification to clear vital sea lanes. ALMDS is designed with four receivers and a 50W class 532nm Nd:YAG laser. ALMDS is currently in low rate initial production with the prime contractor, Northrop Grumman. The second system is the Electro-Optic Identification (EOID) is a mine identification system that is a component of AN/AQS-20A tow body. A sonar on the tow body cues the EOID to image potential threats. The EOID also uses Areté's STIL technology and can be used to generate high resolution 3-D images of mines and other ocean bottom objects. In 2002, two units of EOID were delivered to Raytheon, the prime contractor with both units

arriving on-time and on budget. There were four additional deliveries of EOID in 2004-2005, and two production units were delivered to Raytheon in 2007. Areté is under contract to deliver another 9-lot of the 11 unit initial buy with the new production Primus laser.

An imaging STIL lidar system can also be developed for capturing laser-induced fluorescence imagery. With minor changes to the transmitter and receiver optics, the system operates in a number of different modes including 3D multispectral, hyperspectral, multi-excitation hyperspectral, and fluorescence-lifetime hyperspectral. All of these sensor functions provide discriminating capabilities for targets exhibiting spectral fluorescence signatures (Gleckler *et al.* 2001).

5.8 Laser Line Scanner

Laser Line synchronous Scanning (LLS) have been used in underwater imaging for decades. LLS sensors reduce the detrimental effects of backscatter and blur/glow/forward scatter by producing imagery from a very small laser spot and a small receiver field-of-view footprint. The principle is based on a thin laser beam reflected by a rotating mirror so that it scans the sea floor in a direction perpendicular to platform motion. A sensitive set of receive optics is “synchronously scanned” so that only light from a small area of the sea floor which has mostly not been scattered Jaffe *et al.* 2001. The Laser Line Scan system is a towed laser system that produces high-resolution “picture quality” panoramic image surveys at rapid coverage rates. The transmitted and reflected laser beams are swept through a 70° sector, building an image pixel by pixel in each scan line.

LLS produces higher resolution images than side-scan sonar but at the cost of surface coverage. The coverage rate depends on the operational height above bottom which in turn is dictated by the water quality. LLS has proven useful for ground-truthing selected portions of a broad-scale side-scan sonar data set over a variety of applications, including habitat and fisheries assessments, and underwater search and recovery operations. Though the LLS provides somewhat lower resolution than video or still photography, it is capable of providing a coverage range that may be up to four or five times greater than video (Waddington and Hart 2003). Some articles about LLS systems are discussed by Moore *et al.* (Moore *et al.* 2000).

5.9 Polarisation Imaging

Examples of active hyperspectral imaging combined with polarisation imaging has been developed by Thales (then Thomsson CSF) (Clemenceau *et al.* 2000). In the work by Clemenceau *et al.*, a polarization active (laser) imager built at CREOL showed some strong capabilities for the detection of metals. Their work investigated the dependence of polarisation on the angle of incidence. In a paper by Morvan *et al.* at Thales (Morvan *et al.* 2004), a multispectral polarization active imaging concept is presented. The acquisition, at different wavelengths, of images coded in intensity and in degree of polarization ($0\% < D_p < 100\%$) enables to get information about the spectral signature of targets as well as their polarization properties. A theoretical analysis and an experimental validation of this technique are presented. Performing multispectral polarimetric imaging increases identification and recognition capabilities. In particular, isolating surface and volume scattering is a convenient way to identify, on the one hand surface nature and roughness of a target and, on the other hand, spectral characteristics of its paint.

New publications of polarization relevant for underwater imaging include Zhou *et al.* (Zhou *et al.* 2009). Polarization characteristics of coastal waters were recently measured using a new Stokes vector instrument developed by the Optical Remote Sensing Laboratory at CCNY. The measured degrees of polarization (DOPs) and normalized radiances as a function of angle and wavelength match very well with simulated ones obtained with a Monte Carlo radiative transfer code for the atmosphere-ocean system. It is

shown that the visibility can be improved for unpolarized target by placing a polarizer oriented orthogonally to the partially polarized direction of the veiling light before camera. The blurring effects strongly depend on the small angle scattering in the forward directions. For polarized targets the Monte Carlo simulation of slab geometry for polarized pencil light shows that the scattering medium has a very strong ability to retain the polarization status of the incident light, which can be utilized to improve the image contrasts for targets with very different polarized reflection properties.

5.10 Laser Induced Fluorescence

Laser induced fluorescence has been investigated for a number of years in atmospheric, land vegetation and aquatic remote sensing. In contrast to free atoms and molecules, solids and liquids exhibit broad emission and absorption spectra. A laser with a fixed wavelength can excite solids and liquids due to this broad absorption. Following the excitation, there is a fast (picosecond) radiation relaxation down to the lowest level of the excited states where the molecule rests during a typical life time on the order of ns. The decay from this low excited state then occurs down to various sublevels of the ground state giving rise to the emission spectrum characteristic for the molecule at hand. The life time is also an indicator for the type of molecule involved. By varying the excitation wavelength a characteristic excitation spectra can also be obtained.

5.10.1 Example of Systems and Studies of Fluorescence

Stute *et al.* measured fluorescence spectra in a tank trial (Stute *et al.* 2002) with the attribution of components known from literature. To have a rough classification, they used wavelength regions according to: elastic scattering 528 nm - 536 nm, fluorescence of CDOM (coloured dissolved organic matter) 560 nm - 630 nm, Raman scattering 638 nm - 662 nm, fluorescence of Chlorophyll-a 670 nm - 690 nm.

An example of an enhancement of a LLS system is the FILLS system (Fluorescence Imaging Laser Line Scan) (Jaffe *et al.* 2001). It is a colour version of the LLS that permits up to four different wavelengths in the receiver system. Each receiver consists of a rotating input optical assembly, a controllable aperture assembly, a photo-multiplier tube, a preamplifier and signal conditioning electronics, and an analog-to-digital converter. The four rotating input optical assemblies and a rotating output optical assembly are mounted on a drive shaft to ensure mechanical synchronization of the laser spot and the receiver spots across the sea floor. The input/output optical assemblies employ four-faceted mirrors, yielding four 90-degree scan lines per rotation of the drive shaft. Scan line (cross track) imagery is formed from the centre 70-degree portion of each scan line by digitizing the electrical output from each receiver to 12 bits at a user selectable (512, 1024, 2048, or 4096) number of pixels per scan line. Two-dimensional imagery is formed by platform motion, ensuring that successive scan lines are displaced from each other. The sensor can be configured in several ways to acquire different types of data. In the Fluorescence Imaging Laser Line Scan (FILLS) configuration, the laser is an Argon Ion laser with its output tuned to 488 nm, and the four receivers are fitted with interference filters centered at (for example) 680 nm, 488 nm, 515 nm, and 570 nm respectively. In this configuration, channel 2 images with elastically scattered light, while channels 1, 3, and 4 image with red, green, and yellow light, respectively. The source of this red, green, and yellow light is predominantly natural fluorescence stimulated by the 488 nm laser light. (However, because of their spectral proximity, there is some "leakage" of the elastically scattered 488nm light into the green channel image.) In a second configuration, the laser can be an Argon/Krypton mixed gas laser, which produces simultaneous outputs at 647nm (red), 515nm (green), and 488nm (blue). When three of the receivers are fitted with matching filters, the data required to produce RGB colour imagery can be obtained. In this configuration no filter is installed in the remaining channel. In the FILLS-configuration the sensor can present remarkable fluorescence characteristics of a coral environment.

Certain hard coral species give relatively strong green and/or yellow fluorescence signals. Soft corals typically give relatively strong red fluorescence signals. In addition, the carbonate sediment gives a lower level of fluorescence in all three fluorescence channels. The high gain capabilities of the PMTs are required in order to produce good FILLS imagery, particularly in the red channel. First, the fluorescence signal levels are markedly lower than the elastic scatter signal levels. Second, the large absorption coefficient of water in red leads to strong attenuation of the already weak fluorescence signal. For this reason, the red channel was almost always run at maximum gain, and better red fluorescence imagery is obtained at lower scanner RPMs. Another environment that yielded interesting FILLS imagery was of stromatolites near Lee Stocking Island in the Bahamas. When stimulated by the 488nm laser light, the stromatolites produce significant red fluorescence signals. This imagery was acquired at a 5 knots tow speed and a scanner speed of 2000 RPMs. The tow body altitude was 4.5 meters, and its depth was 1 meter.

The *Italian group from ENEA* have built several laser induced fluorescent (LIF) lidar systems and shown interesting results (Barbini *et al.* 2006; Barbini *et al.* 2005; Fantoni *et al.* 2004; Barbini, Colao, Fantoni, Frassanito *et al.* 2000). One of the goals have been to monitor the vertical concentration profiles of organic substances and phytoplankton. By measuring the time resolved lidar signals the depth profiles of concentration of different substances and other seawater parameters can be extracted. The lidars are aimed for manned vessel or ROV operation.

In the paper by Fantoni *et al.* (Fantoni *et al.* 2004) a lidar fluorosensor payload for submarine investigation (ROV) is described together with a design for a new lightweight flying payload for large surface monitoring to be installed on an unmanned aerial vehicle (UAV). There are many applications for these kind of instrument like monitoring of Chlorophyll-a (Chl-a) concentrations for estimate of the bio production. Other substances include oil and industrial waste products including dangerous organic pollutants (PCB, dioxins, PAH) as well as anthropogenic discharges (DOM and detergents). The data from this instrument can help calibration of satellite radiometric observations supply important complementary data to concurrent surveys by local (video cameras) or remote techniques. The carbon cycle is among the more important global phenomena affecting the Earth's climate. There is a large interest to study the phytoplankton dynamics, since such phenomena are thought to be responsible for the sequestration of atmospheric carbon dioxide, one of the most important greenhouse gases. Satellite data offers a vast coverage over large waters which are hard to reach by other means like the Antarctica. It is therefore of importance to calibrate the satellite radiometer data related to chlorophyll production estimates. A ROV base fluorescence lidar offers such a possibility to obtain depth resolved chlorophyll concentration profiles.

The results from the ENEA lidar (Barbini *et al.* 2006; Barbini *et al.* 2005) indicate that the satellite sensor SeaWiFS over-estimates high concentrations and underestimates low concentrations of chlorophyll. In order to correct this behaviour, the Chlorophyll-a bio-optical algorithm of SeaWiFS has been recalibrated according to the measurements of ELF (ENEA Lidar Fluorosensor), thus providing a new estimation of the primary production in the Southern Ocean.

Professor Reuters group from the University of Oldenburg and Dr. Karpicz *et al.* from the University of Vilnius have developed hydrographic lidar systems based on fluorescence (Karpicz *et al.* 2006; Barth *et al.* 2000; Zielinski *et al.* 2000; Harsdorf *et al.* 1999). The detection of distinct events like harmful algae blooms or transport of chemicals and other pollutants with the water masses is of special interest for the coast guards. Passive optical radiometers on-board satellites show remarkable results in detecting, for example, the chlorophyll distribution over the open ocean. However, in coastal areas the algorithms for discriminating phytoplankton contents in the water from colour ratios must carefully consider other water constituents like gelbstoff (or CDOM - Coloured Dissolved Organic Matter) and suspended particles. This results in a much more complex theory of radiative transfer and, consequently, in larger uncertainties (Zielinski *et al.* 2000). An additional

serious problem for the North and Baltic Seas for example, is the high cloud probability during the year which inhibits the gathering of continuous information on hydrographic parameters by spaceborne techniques over a large area. Some of the arguments above have motivated German areas of jurisdiction in the North and Baltic Seas to operate airborne survey for maritime pollution since 1985 (Zielinski *et al.* 2000). Two Do 228-212 aircrafts were used, especially equipped with side-looking airborne radar (SLAR) for detecting oil slicks over large distances and ultraviolet (UV) as well as infrared (IR) line scanners for mapping the sea surface in the nadir range. One of these aircrafts, operating around the clock, was additionally equipped with a microwave radiometer (MWR) and a mapping laser fluorosensor (LFS). These sensors allowed for a more detailed analysis of oil spills in terms of film thickness, and hence discharged volumes. The LFS used a XeCl excimer laser as an active radiation source in the UV (at 308 nm). It detects the spectral fluorescence signal emitted from the upper water column and can yield information on the type and quantity of the spilled substance. Moreover, hydrographic parameters such as gelbstoff, chlorophyll in phytoplankton, and seawater turbidity can be measured (Zielinski *et al.* 2000). The LFS, is designed with two high energy pulse lasers in the UV at 308 nm (XeCl excimer laser, 150 mJ pulse energy, 20 ns pulse length) and 383 nm (dye laser, 20 mJ, 15 ns). The stimulated fluorescence as well as the scattering of the laser light at the water surface and within the water column are detected with a 20 cm telescope and then spectrally separated into 12 detection channels (detection wavelengths at 332, 344, 365, 382, 407, 441, 471, 492, 551, 592, 650, and 684 nm with a typical optical bandwidth of 10 nm). The operational altitude is between 100 and 300 m resulting in a surface swath width of 150 to 450 m, utilizing a conical scanner. The main features of the laser fluorosensor in its original design for oil spill measurements are:

- estimation of oil film thickness between 0.1 and 10 μm ,
- calculation of the oil volume on the water surface,
- identification and classification of the oil through its spectral signature,
- discrimination between natural and mineral oil films and
- detection of oil below the water surface.

Harsdorf *et al.* (Harsdorf *et al.* 1999) describes a the submarine lidar, combining a range-gated imaging device and a fluorescence lidar. A q-switched Nd:YAG laser is used as the common light source. They concluded that the expanded frequency-doubled laser pulse the gated CCD camera is particularly useful for recording images of damaged containers with chemical cargo where harmful substances might be released into the water column. Tuned to UV emission, the same laser was used for remotely classifying fluorescent substances spreading on the seafloor. Analysis of emission spectra allowed to distinguish between natural substances, e.g. yellow substance and pollutants. The system uses a linearly polarized laser which may provide additional information about water column, object and background. A method for backscatter rejection next to range-gating is a polarization technique where the difference between target and background depolarization characteristics is utilized to enhance the image.

Karpicz *et al.* (Karpicz *et al.* 2006) describe an oil spill detection fluorosensing lidar for onshore or shipboard operation. Some difficulties for its operation arise from the inclined path of rays. This is due to the increased reflection of the laser beam at the air–water interface, the decreased fluorescence signal, and the increased background light when compared with other instruments having a close-to-nadir measuring geometry. They analyze the loss in fluorescence signals due to geometry and waves. At FOI we have presented (Tulldahl and Pettersson 2007) simulated and experimental data from underwater target detection with an incidence angle of 5 degrees which has some connection with the lidar discussed by Karpicz *et al.* (Karpicz *et al.* 2006). The application of such a lidar was aiming at the detection of shallow underwater objects. Small underwater objects such as vehicles and divers can pose threats to fixed installations and ships. For ships, these threats are present both at sea and in harbours. Shallow underwater

targets, including drifting mines, are difficult to detect with acoustic methods and thus complementary methods are required. For sensing from a ship or from land, optical detection can be highly improved by use of a pulsed laser system.

Karpicz *et al.* (Karpicz *et al.* 2006) also propose a fluorescence data processing method that efficiently eliminates the background water column fluorescence from signals, such as yellow substance. This enables oil fluorescence to be distinguished from variable natural water fluorescence.

Over the past decade, laser-induced fluorescence (LIF) of plants has been explored as a tool in land vegetation studies. Compared to reflectance, LIF, and particularly (ultraviolet) UV-induced fluorescence, may be a more accurate indicator of the physiological state of plants and may be able to detect the impacts of environmental stresses on them at earlier growth stages (Samson *et al.* 2000). It should be noted though that UV-induced fluorescence is of limited use in water because of the high attenuation at these wavelengths.

Bensky *et al.* recently observed instantaneous fluorescent emission from Chl in phytoplankton resident in vitro seawater samples as a result of pumping with a 440 nm, 70 ns laser pulse (Bensky *et al.* 2008). Delayed fluorescence of 10 ± 2 ns is seen, and a functional cross section of 0.0095 \AA^2 is derived from the data.

A method for the characterization of phytoplankton species, based only on the analysis of Chlorophyll-a fluorescence peak, is described by Mochi *et al.* (Mochi *et al.* 2002). The method was tested on pure monocultures in the laboratory by using a high spectral resolution fluorescence lidar.

LDI is an Estonian private corporation, operating in the area of research, development, manufacturing and application of laser-based instrumentation. LDI offers on-line, in-situ, airborne, contact and remote analytical sensors to address environmental, industrial and bio-medical issues, together with a range of software products that control measurements and handle data (<http://www.lidi.ee>). The FLS-A (Fluorescent Lidar System – Airborne) is part of the LDI series of remote laser spectrometers. The FLS-A is optimized for operation onboard aircraft (including helicopters) to provide rapid analytical screening of wide areas of land and water. This data are processed and displayed in real-time, geo-referenced findings constitute in-flight report. The data are archived for post-survey analysis.

The present upgraded version of the ENEA Lidar fluorosensor, aimed to monitor the phytoplankton activity by means of the pump and probe technique, is equipped with a suitable (UV-visible) single/double pulse laser transmitter (ENEA patent pending), send/receive optics and a detection system operating in the spectral resolved mode. The pump-and-probe technique has been developed and adopted to identify sensitive physiological indicators of plant health, which would be less affected than the spectral ratios by the environmental conditions and more suitable to remote application than the time resolved studies. The technique requires to send a saturating laser pulse (the pump) followed by (after a few tens of microsecond) a probe pulse on the same vegetation target. The red Chlorophyll fluorescence emission (@ 690 nm) is detected as induced by the probe pulse alone or in the presence of the pump. In the latter case, having the pump laser already saturated, all the reaction centres, and the fluorescence emission is maximal for a healthy vegetation tissue.

The pump and probe technology was invented by the NASA lidar group at Wallops Island (Chekalyuk *et al.* 2003). It provides remote measurement of phytoplankton photosynthetic variables along with pigment and organic matter fluorescence, down-welling and up-welling hyperspectral measurements and sea surface temperature. The utilization of an airborne platform provides for rapid remote characterization of phytoplankton photosynthetic activity, biomass and diversity over large aquatic areas. The pump and probe (P&P) lidar technique is one of the first practical implementations of ‘superactive’ remote sensing.

Porykova *et al.* (Poryvkina *et al.* 2000) discuss monitoring of large water areas or temporary processes in a spot area. The most productive way is thought to be a balanced combination of *on line* continuous fluorescence measurements and sampling (remote sensing) procedures, which allows to decrease the time-consuming manual analysis of water samples in the laboratory.

Maslov *et al.* (Maslov *et al.* 2000) describe a shore (or ship based lidar) used for under water monitoring which can play a key role in developing a system for continuous express monitoring of coastal seawater areas. The dependencies of an echo-signal (in this case water Raman scattering) on the sensing distance of the laser beam are investigated. The results obtained appear to correlate well with the theory of laser remote sensing under large incidence angles, in which wind waves are taken into account. In the experiments, laser radiation with 532 nm wavelength at 10 Hz repetition rate, with 10 ns pulse duration and 10 mJ pulse energy was used. The sensing distance was up to 100 m at a sensing angle of approx. 80°. The possibility of increasing the sensing distance up to 0.5-1 km is shown.

Brown and Fingas (Brown and Fingas 2003) review laser fluorosensors for oil spill monitoring and come to some conclusions, probably relevant for many other laser fluorescent applications as well. The most important conclusions were:

- To facilitate the cost-effective “operational” use of laser fluorosensors, there is a need to develop lightweight, high-powered, high-repetition rate, solid-state ultraviolet lasers. These smaller lasers can then be employed in smaller twin-engine aircraft and perhaps ultimately in unmanned aerial reconnaissance vehicles.
- To improve the sensitivity for the detection of all classes of oil, a variety of laser excitation wavelengths is required. At the present time, most laser fluorosensors used for oil detection operate at 308 or 355 nm, which is a compromise that allows for the detection of all classes of oil (light refined, crude and heavy refined products). The cost of this compromise, however, is reduced sensitivity for certain classes.

5.11 Laser Induced Breakdown Spectroscopy

The Laser-Induced Breakdown Spectroscopy (LIBS) technique (Barbini, Colao, Fantoni, Lazic *et al.* 2000) is based upon the analysis of the atomic emission lines generated close to the surface sample. The emission is observed once a laser pulse is focused on the surface, where the very high field intensity initiates an avalanche ionization of the sample elements, giving rise to the so-called breakdown effect. Spectral and time-resolved analysis of this emission are suitable to identify atomic species originally present at the sample surface. Using fiberoptics to guide the laser exiting beam close to the target under investigation simplifies the use in water. New techniques in LIBS involves double pulses to increase efficiency (Nassef and Elsayed-Ali 2009). Few applications have involved the use of LIBS in underwater systems so far.

5.12 Raman Techniques

Raman spectroscopy have been used since many decades in remote sensing applications especially for atmospheric lidar. We will just give one single example for illustration. A compact remote Raman spectroscopy system of potential interest for EMMA was developed at NASA Langley Research Center and has demonstrated its ability to identify chemical composition of various rocks and minerals, leaves and fossil samples (Garcia *et al.* 2009).

The NASA Raman sensor utilizes a pulsed 532 nm Nd:YAG laser as excitation source, a 4-inch telescope to collect the Raman-scattered signal from a sample several meters away, a spectrograph equipped with a holographic grating, and a gated intensified CCD (ICCD) camera system. Time resolved Raman measurements were carried out by varying the gate delay with fixed short gate width of the ICCD camera, allowing measurement of both

Raman signals and fluorescence signals. Rocks and mineral samples were characterized, including marble, which contains CaCO_3 . Analysis of the results reveals the short ($\sim 10^{-13}$ s) lifetime of the Raman process and shows that the Raman spectra of some mineral samples contain fluorescence emission due to organic impurities. Also analyzed were a green (pristine) and a yellow (decayed) sample of leaves. It was observed that the fluorescence signals from the green and yellow leaf samples showed stronger signals compared to the Raman lines. It was also observed that the fluorescence of the green leaf was more intense and had a shorter lifetime than that of the yellow leaf. For the fossil samples, Raman shifted lines could not be observed due to the presence of very strong short-lived fluorescence.

5.13 Conclusion and Comments for Imaging Systems

Above we have exemplified some underwater imaging techniques such as range gated imaging, laser line scanning (LLS), Streak tube imaging lidars (STIL), multi/hyperspectral techniques, polarization imaging and others. Which technique is the best and most cost effective depends of course on the application. Numerical simulations of the relative performance of streak-tube, range-gated, and PMT-Based Airborne imaging lidar systems with realistic sea surfaces has been investigated by DeWeert *et al.* (DeWeert *et al.* 1999). The resulting images realistically simulate the refractive effects of the ocean waves. They demonstrate the excellent contrast of a STIL for high resolution image classification. However, the superior energy utilization of the range gated approach, makes it a better method for airborne lidar imaging, with an advantage that grows exponentially with depth. Likewise, a compact rectangular array of time-resolved pixels perform search tasks better than does a STIL.

Hou and Weidemann recently published an interesting paper on diver visibility (Hou and Weidemann 2009). They discussed the effects of turbulence on underwater imaging and demonstrate that the previous diver visibility model based only on particle scattering can lead to erroneous predictions under certain conditions. When the accumulative effects of turbulence scattering is included, by using the general underwater imaging equation which is based on Kolmogorov power spectrum, they were able to explain the observed discrepancy, assuming weak path radiance contribution.

6 Platforms

Platforms will continue to be developed for autonomous operation with the long term aim to reduce cost of operation and limit manpower involvement. Both underwater, surface and airborne platforms are included in this development. Below we give some recent examples on platforms of relevance for seabed monitoring. This will include in-water systems as well as unmanned surface vessels and unmanned aerial vehicles. Also, some examples of used sensors are given.

6.1 Autonomous Underwater Vehicles (AUV) and Gliders

One new type of is called the Bottom Stationing Ocean Profiler (BSOP) (Fefilyatye *et al.* 2009), and is an un-tethered, autonomous platform that stations itself on the sea floor and ascends to the surface at specific time intervals or, when triggered by certain events such as recognizable acoustic signals, collected and analyzed on board. The system is autonomous and is designed to remain in the ocean for extended periods up to two months. When triggered by certain events such as recognizable acoustic signals, the systems moves to the surface where it is designed to take video and imagery of the surrounding ocean surface and analyze it for the presence of ships, thus, potentially enabling automatic detection and tracking of marine vehicles as they transit in the vicinity of the platform. Data is sent to the ground control via bi-directional RF satellite link and can have its mission parameters reprogrammed during the deployment. The described unit is low cost, easy to deploy and recover.

A new type of unmanned slowly moving ROVs are called gliders (Schofield *et al.* 2009) and they are anticipated to have a great impact on marine monitoring. The long duration and low costs of gliders allow them to anchor spatial time series. Large distances, over 600 km, can be covered using a set of alkaline batteries. Lithium batteries can anchor missions that are thousands of kilometres in length. A wide range of physical and optical sensors have been integrated into the glider allowing measurements of temperature, salinity, depth averaged currents, surface currents, fluorescence, apparent/inherent optical properties active and passive acoustics. A command/control centre, entitled Dockserver, has been developed that allows users to fly fleets of gliders simultaneously in multiple places around the world via the Internet.

6.2 Unmanned Surface Vessels (USV)

Unmanned surface vessels (USV) are now becoming used for environmental monitoring. Functionally, they are much simpler than an autonomous underwater vehicle (AUV) yet quite versatile for the kind of missions they are able to perform. Several USV projects are in existence on the international arena.

One example of USV is developed by Harbor Wing Technologies (<http://www.harborwingtech.com/products.htm>). The open-ocean vessel is fitted with a hard airfoil sail and suited for long range, long duration missions. Another example is the Israeli Protector systems, highly autonomous and remotely controlled, the Protector can successfully monitor waterways with general guidance from a commander and operator at sea or from shore. The unmanned Protector has an on-mount camera allowing for day and night operation and has a forward-looking infrared laser range finder capability to detect and track targets in the near vicinity. The Boat Control unit's navigation sensors are used to obtain location, speed, heading and course data. The communications unit maintains a constant link between Protector and the control station.

6.3 Unmanned Aerial Vehicles (UAV)

A final example of monitoring platforms and systems of interest for remote sensing are based on UAV:s. UAV-borne sensors make it possible to achieve high surface coverage. If the UAV is a small helicopter, and hence has vertical take-off and landing (VTOL) capability, it is possible to combine high surface coverage rate with the possibility to stop and look at specific objects at reduced height to get a higher resolution. The state of the art in line of sight stabilization for gimbals is in the order of 10-20 μ rad which means a resolution on the ground of about 0.2-0.4 cm from 200 m altitude, which would be the normal height when high surface coverage rate is needed. UAV's with VTOL-capability have the advantage that they only need a very small take-off and landing sites. They are very mobile without needs for special launch and recovery equipment.

Skeldar (http://www.saabgroup.com/en/ProductsServices/products_az.htm) is a fully autonomous, mobile system with VTOL capacity, see Figure 5. Its modular design makes it possible to choose between different payloads. The UAV Control Station is modular and can be customized and adapted for integration into other systems and configurations. No launch or recovery equipment is needed and operation requires only a few staff (four). The Skeldar can hover in a fixed position for hours and easily hide behind structures, operate close to other objects and perform exact manoeuvres repeatedly.

The structural material for the fuselage is carbon fibre, titanium and aluminium composite. The engine, that can be customized, runs on petrol or heavy fuel. The power train consists of a robust drive shaft with a centrifugal clutch that relays the power to the rotor system via a drive belt and a main gearbox. The main rotor uses a Bell-Hiller configuration system comprising stabilizer bar and paddles. Avionics include redundant computers, GPS receivers, inertial measurement unit (IMU), air-data system and magnetic heading indicator allowing fully autonomous operation while maintaining total radio silence.



Figure 5. The UAV helicopter Skeldar from Saab Aerosystems.

The communication between the vehicle and the UAV Control Station UCS is achieved via highly secure direct links containing sensor and command and control data. Sensor data and command and control are transmitted via separate communication links. The vehicle is designed to carry a range of COTS payloads such as EO/IR, SAR and EW sensors. The system is also ready for integration of future sensors and upgrading.

APID 55 from CybAero (<http://www.cybaero.se/>) is a fully autonomous multipurpose VTOL UAV, see Figure 6. The vehicle has on-board systems for navigation and stabilization. It can carry out fully autonomous mission with total radio silence.



Figure 6. The UAV helicopter APID 55 from CybAero.

The APID system consists of three different components: the APID 55 UAV, a Ground Control Station and an optional Payload System. The helicopter is designed to carry a wide range of payload equipment such as: stabilized cameras, IR sensors, laser scanners, antennas and other equipment. The GCS is the work station for the vehicle operator who controls the vehicle and for the operator who controls the payload. Information and data in the GCS can be presented and logged.

Both the APID 55 and Skeldar are small unmanned helicopters which are capable of starting, landing and flying autonomously, without people on the ground providing real time support for flight control or navigation. Both helicopters have landing facilities that make it possible to land on very small sites. Representatives from CybAero (APID 55) claim that it even would be possible to land on the back of a ground vehicle. They have an ongoing development program aiming at that ability. With that ability the access to the VTOL UAV would be very high. Representatives from SAAB Aerosystems (Skeldar) have some doubt on landing on such a small site. Skeldar normally requires a site with 10 m diameter, it can however manually be landed with high precision. The Skeldar system comprises two helicopters and they claim that the availability of one helicopter in the air is better than 85 %.

Wingless UAV's are often regarded as more demanding on maintenance than fixed-wing UAV's, but both companies stress that maintenance no longer is any problem. These UAV's are small and they are difficult to detect visually at ranges beyond 0.5 km, detection by sound is less than 1 km for Skeldar. Personnel involved in handling and flying these UAV's is typically four; one UAV-commander and mission planner, one payload-controller/intelligence evaluator and two technicians responsible for ground data equipment and maintenance.

Table 1. Comparison of specifications for the UAV helicopters Skeldar and Apid 55.

Parameter	Skeldar	APID 55
Total length (incl. rotor disc):	4.0 m	4.0 m
Height:	1.3 m	1.2 m
Width:	0,95 m	0.95 m
Rotor diameter:	3.3 m	3.3 m
Empty weight:	150kg	105 kg
MTOW (incl. payload and fuel):	200 kg	160 kg
Power rating:	41 kW	41 kW
Max speed:	> 130 km/h	90 km/h
Endurance:	3-5 hr	3-6 hr
Service ceiling:	3500 m	3000 m
Available payload power:	~ 0,5 kW	0,7 kW

The US Navy has an airborne mine detection program called Cobra (http://www.minwara.org/Meetings/2007_05/Presentations/TH1000MINWARA_Conference_2007_Breaching_10May07.pdf). The main sensor in the Cobra program is called Rapid Overt Airborne Reconnaissance (ROAR) (Moran *et al.* 2003). ROAR is an advanced active LIDAR system for UAV airborne littoral mine, minefield, and obstacle detection and localization. It has a number of desirable features such as wide search (200 m) from 3000 ft altitude using cm-class range resolution. This is accomplished by a combination of active and passive multispectral imaging with high 3-D range resolution. The mines shall be detected and localized in very shallow water (VSW: 10 ft to 40 ft depth), in the surf zone (SZ: 10 ft to mean high-tide line) as well as the beach zone (BZ).

ROAR is of principal interest for the EMMA project since it combines passive EO with a high-resolution 3-D lidar. The latter is accomplished with a 512×512 recently developed high-sensitivity gated FPA (<http://www.litecycles.com/3Dreceiver.htm>) with cm range accuracy. The scanner sweeps are of 200×20 m² for underwater detection and 200×60 m² over land. The scanner allows multiple looks, is gimbal stabilized and can track a point in space for studying details. The laser is capable of emitting three wavelengths out of which one is green, in order to enable water penetration. The stated volume, weight and power requirements are 2 ft³, 250 lbs and 2.5 kW, respectively. Figure 7 shows examples of system characteristics.

Another interesting type of UAV:s are small and lightweight vehicles which can be operated at low costs. SmartOne (<http://www.smartplanes.se/>) is one example of such a UAV constructed for forestry and agricultural applications (Figure 8). The platform is constructed to withstand the heavy pounding associated with use in the forest environment. The UAV system is small and light enough to be carried and operated by one person. The aircraft carries a calibrated compact camera and weighs in total close to 1.1 kg.

In 2009, the SmartOne UAV was tested in a survey of shallow bottoms in the Interregional project ULTRA (http://www.kvarken.fi/Pa_svenska/Projekt/Ultra). The survey was made by the company PIEngeering (<http://www.pieneering.fi/>) in a part of the Rönnskär archipelago, Finland. Data analysis from this survey has however not been performed yet.

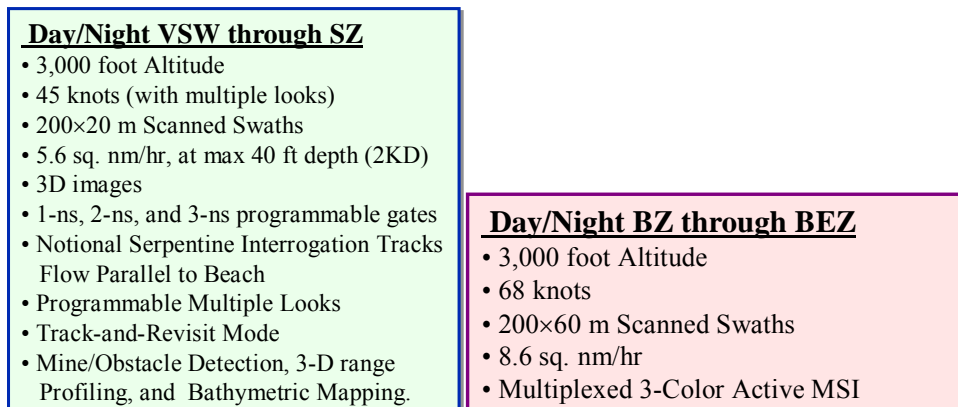


Figure 7. Main specifications for ROAR. Source: LiteCycles.



Figure 8. The small UAV SmartOne by SmartPlanes (<http://www.smartplanes.se/>). The photo is taken at the occasion for a survey of shallow bottoms in the Interregional project ULTRA (http://www.kvarken.fi/Pa_svenska/Projekt/Ultra).

7 Performance Estimates for Airborne Scanning Lidar Concepts

We will estimate the performance of potential lidar systems for underwater observation. The examples are mainly aiming at airborne systems. We investigate a few type of systems concerning laser and receiver characteristics vs size, weight and power (SWaP) coupled with the performance parameters such as maximum range, coverage rate, spectral and range resolution etc.

The sensor concept is based on a traditional depth sounding lidar using manned aircraft. The system is complemented with and a smaller system to fit a UAV and also with a high resolution imaging camera using time gating to enhance water penetration as compared with passive EO cameras. The performance estimates will be of the “back of the envelope type” to assess the realization potential. Table 2 specifies the range of the most important optical parameters in a scanning bathymetric lidar system.

Table 2. Typical parameter range for airborne bathymetric lidar scanners.

Parameter	Value	Comments
Spatial resolution IFOV per pixel.	N soundings/m ²	Today N=1-8 is state of the art for bathymetry
Laser divergence	> IFOV	IFOV=Instantaneous field of view
Temporal resolution	About 100 ns for imaging	Gating reduces background light for imaging ns resolution for depth sounding
Emitted wavelengths	0,4-0,8 μm	Filtered by the water column if not detected by water surface emission
Laser Wavelength	UV-visible	Could be used in a multi spectral configuration, RGB is one possibility for reflectivity. UV may be needed for some fluorescence
Laser pulse energy	Varies , mJ or more /pulse	
Laser prf	Varies	Adopted to search rate , typical 100-1000 Hz
Laser pulse time	< 5 ns for depth sounding	May be longer for reflectivity/fluorescence imaging
Spectral resolution	Typical 2 nm	Optical band pass filter in relation to laser line and throughput
Noise equivalent power per pixel, NEP W	nW level	For depth receiver typically 1-250 nW Depending on daylight level For imaging mode it can be smaller
Diameter receiving optics	Varies depending on platform (manned or unmanned)	Typically 0.1-0.2 m
Detector array	n*n	n=1-4 for depth sounding and large (>128*128) for high res. imaging

In order to estimate the performance from an airborne lidar we follow the formalism by Measures (Measures 1984) but with some small changes in notation. The signal-to-noise ratio (SNR) for target or bottom detection is given by

$$SNR_T = \frac{P_r}{NEP} = \frac{P_L \cdot \xi_L \cdot \xi \cdot G \cdot A_r}{NEP \cdot (n_w R + D)^2} \cdot \exp\left(-2 \int_0^D K(z) dz\right) \cdot T_{atm}^2, \quad (1)$$

where P_r is the received optical power from the bottom, NEP the noise equivalent power of the receiver. In Eq (1), P_L denotes the laser peak power. The factor $\xi_L(R)$ denotes the total system efficiency. Variables R and D respectively denote the sensor altitude and bottom depth. $\xi(R)$ describes the loss obtained when the receiver FOV does not cover all the upwelling reflected laser light, this happens during day time when it is optimal to reduce the receiver FOV to suppress the daylight. The optimal FOV gives a loss $\xi(R)$ of about 50-70%. $K(z)$ is the system attenuation coefficient vs depth z . Note that the solar induced background noise can increase the NEP from typically 1 nW to 250 nW. G is ρ/π for the return from a bottom with reflectivity ρ_b . For the water backscatter the parameter G can be substituted by $G = \beta_w c \tau / 2$ where β_w is the water backscatter coefficient.

The NEP can be written as the mean square of the different noise currents:

$$NEP = \left[(I_b^2 + I_{bsc}^2 + I_s^2 + I_d^2) M^2 F + I_t^2 \right]^{1/2} / (MR_\lambda), \quad (2)$$

where I_i are the unity gain rms-currents due to the optical background of the scene, atmospheric backscatter, signal shot noise and detector dark current respectively. The RMS-thermal noise current from the detector and preamplifier is I_t and R_λ is the detector responsivity (A/W) at wavelength λ and M the detector gain. F is the so called excess noise factor (*The Infrared & Electro-Optical Systems Handbook* 1993). This factor is relevant for avalanche detectors and depends on detector material and electron amplification. The following formula from EO/IR handbook might be used to estimate F:

$$F = k_{eff} M + (2 - 1/M) * (1 - k_{eff}), \quad (3)$$

with M being the gain and $k_{eff} = 0.02$ for silicon and $= 0.45$ for InGaAs. Typically F falls in the region 1-10.

If we assume that K is constant down to the bottom depth D and assume that the flight altitude $R \gg D$ and small enough ($< 1000m$) to neglect the atmospheric loss T_{atm}^2 we can simplify equation (1) as:

$$SNR_T = \frac{P_r}{NEP} \approx \frac{P_L \cdot \eta_{tot} \cdot G \cdot A_r}{NEP \cdot (n_w R)^2} \cdot \exp(-2KD), \quad (4)$$

where n_w is the refractive index of water (1.33). This equation is directly solvable for the maximum depth D_{max} according to (under the assumption that NEP is independent of R which is true during low light conditions):

$$D_{max} = \frac{1}{2K} \cdot \ln(S_w), \quad (5)$$

with the system constant S_w defined by:

$$S_w = \frac{P_L \cdot \eta_{tot} \cdot G \cdot A_r}{NEP \cdot (n_w R)^2 \cdot SNR_T} \quad (6)$$

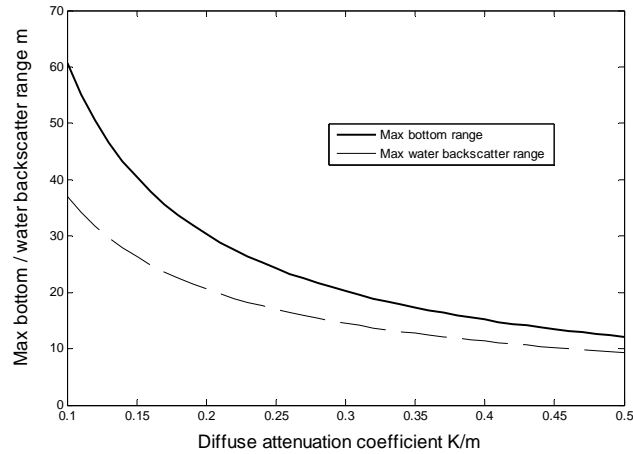
Note that the altitude R is incorporated in S_w and the incremental depth gain ΔD obtained by changing the system factor S_w by a factor F is obtained as:

$$\Delta D = \ln(F) / 2K \quad (7)$$

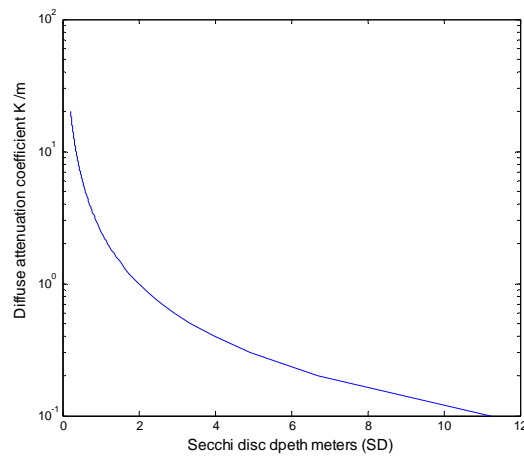
Note the relative small change in bottom range for a large system change (F). For example using $K=0.2/\text{m}$ and $F=10$ we obtain an increase in the bottom range of only about 6 meters. Using the parameters in Table 3 for the depth sounding lidar we can estimate the maximum bottom and water backscatter range vs. the system attenuation coefficient K . One example is shown Figure 9.

Table 3. Example-parameters for a depth sounding lidar

Laser wavelength μm	0.532
Laser pulse energy E_L mJ	10
Laser pulse width τ ns	5
Laser peak power $P_r=E_L/\tau$ MW	2
Overall system efficiency η_{tot}	0.1
Receiver area A_r m^2	0.025
NEP nW	1
SNR_T	7
Bottom reflected normalized intensity G /sr diffuse	$0.1/\pi$
Water diffuse attenuation coefficient K , /m	0.1-0.5
Water backscatter coefficient β	$0.0079 * K^{1.2}$



(a)



(b)

Figure 9. (a) Maximum bottom and water backscatter range obtained by the simplified range equation (5). The noise equivalent power $NEP=1$ nW corresponds to night time operation and the flight altitude of 200 m. (b) The relation between Secchi disc depth SD and K .

For the assumption of limiting solar background inducing detector noise we can estimate the performance according to using the NEP according to:

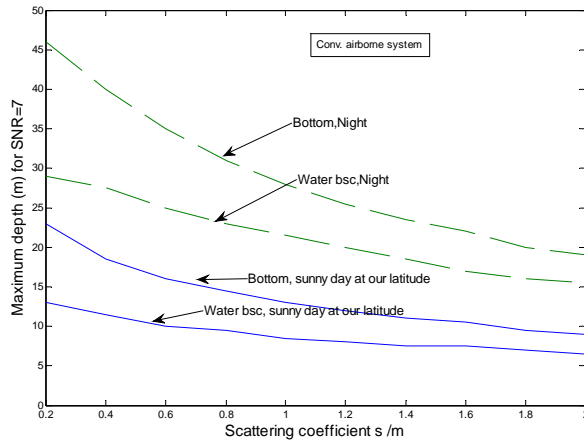
$$NEP = \left[(I_b^2 + I_{bsc}^2 + I_s^2 + I_d^2) M^2 F + I_t^2 \right]^{1/2} / (MR_t) \approx I_b \cdot F^{1/2} / R_\lambda \approx P_b \quad (8)$$

The background noise depends on the optical background power P_b . It can also be calculated from the spectral irradiance and spectral radiant exitance (if it exists) in this case given as:

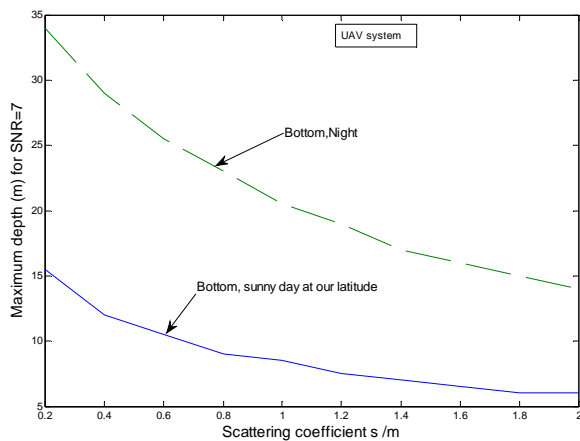
$$P_b = A_r \Delta \lambda \eta_r \Omega_r (\rho_b E_\lambda) \quad (9)$$

where E_λ is the spectral irradiance ($Wm^{-2} \mu m^{-1}$), ρ_b the scene diffuse reflectivity, A_r the receiver area (m^2), Ω_r the receiver instantaneous field of view (sr), $\Delta \lambda$ the spectral filter bandpass (μm) and η_r the receiver transmission. The field of view of the receiver can be optimized during sunny conditions (Feigels and Kopilevich 1999). If we expressions for

this and relations between scattering coefficient s and the diffuse attenuation K and the backscatter coefficient b_b , we arrive at depth ranges vs the scattering coefficient according to Figure 10 where we assumed a conventional manned aircraft system with typical parameters according to Table 3 and with an assumed UAV-borne system where we have lowered the laser pulse energy by a factor 50 (to 100 μJ) to get a small laser system suitable for a UAV.



(a)



(b)

Figure 10. Maximum depth penetration vs the scattering coefficient s for a conventional airborne system with 5 mJ pulse energy (Table 3) and for a potential UAV-borne system with a much smaller pulse energy (100 μJ). Flight altitude 200 m. Note the large difference between sunny and night time conditions.

One interesting application is to have a multicolour capability (e.g. RGB) for the emitting laser. This would enable the measurement of the bottom colour together with the depth. An example of measured spectral attenuation coefficient c is shown in Figure 11. Measurements were made in the Arkö Archipelago on September 12, 2007. As seen in Figure 11, the attenuation for blue and red wavelengths can be higher in coastal waters as compared with that for the green wavelength (532 nm). This in turn will reduce the maximum range at least for a detector-limited system according to equation (5).

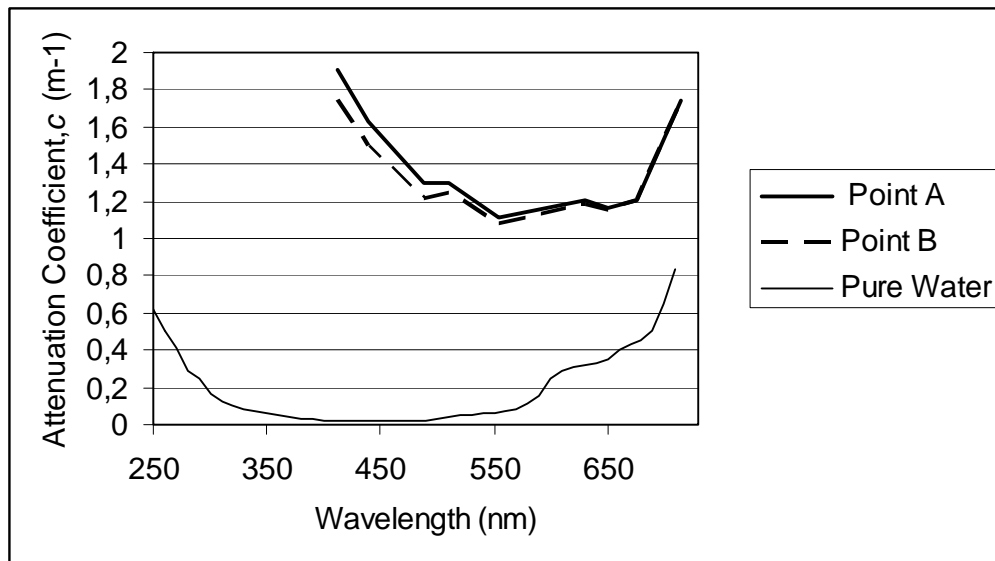


Figure 11. Example of measured spectral attenuation coefficient at nine wavelengths (instrument: AC-9 Wetlabs Inc.) compared to attenuation coefficient of pure water (Mobley 1994). Measurements were made in Arkösund, Sweden on September 12, 2007 at points A and B indicated in Figure 12. The Arkö Archipelago is situated close to the outlet of Motala Ström (Figure 12), a watercourse with a large catchment area transporting large amounts of nutrients and humic substances into the Baltic Sea. This is reflected by a smaller Secchi depth in this area compared to other archipelago areas in the region (up to 2 m smaller Secchi depths in August) (www.motalastrom.org/arsrapporter/2008/alcontrol/PDFer/StoraMSV2008.pdf).

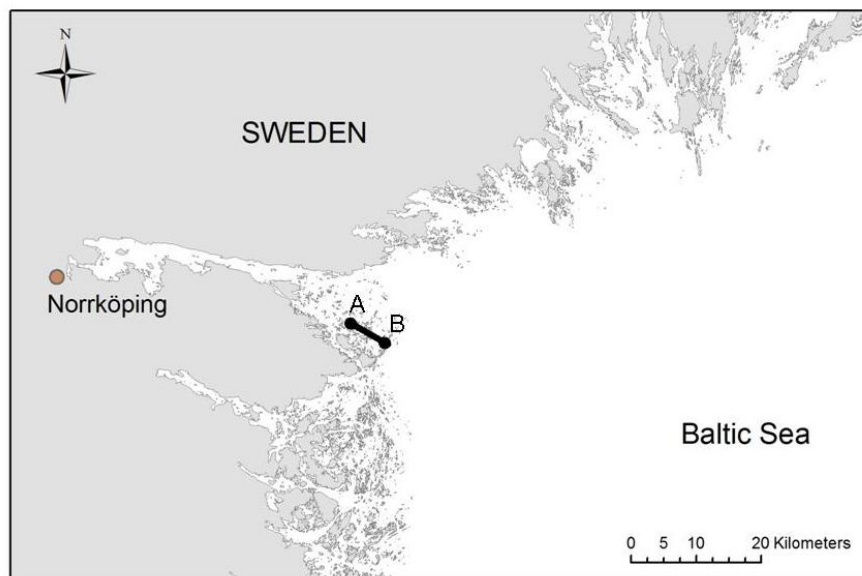


Figure 12. Location of Points A and B for water parameter measurements in Figure 11.

Another possibility is to complement the depth sounding lidar with a time gated high resolution camera allowing imaging details of the bottom to be mapped from the air. In order to estimate the depth loss for an imaging sensor with $n \times n$ detectors as compared with a single detector system we use formula (5) to derive the following

$$D_{\max, n \times n \text{ array}} = \frac{1}{2K} \cdot \ln(S_w^n) = \frac{1}{2K} \cdot \ln(S_w \cdot \frac{NEP}{NEP_n} \cdot \frac{1}{n^2}) = D_{\max, 1} + \ln(\frac{NEP}{NEP_n} \cdot \frac{1}{n^2}) / 2K \quad (10)$$

where we have assumed a detector noise being reduced by a factor q for the pixel noise as compared to the single detector. This reduction q is due to the time gating and small pixel of a gated imager. A reasonable estimate the q can be as low as 10⁻³ for a short gate. Figure 13 shows the estimated depth loss for an N*N gated imaging systems relative a conventional depth sounding single pixel lidar for different values of K.

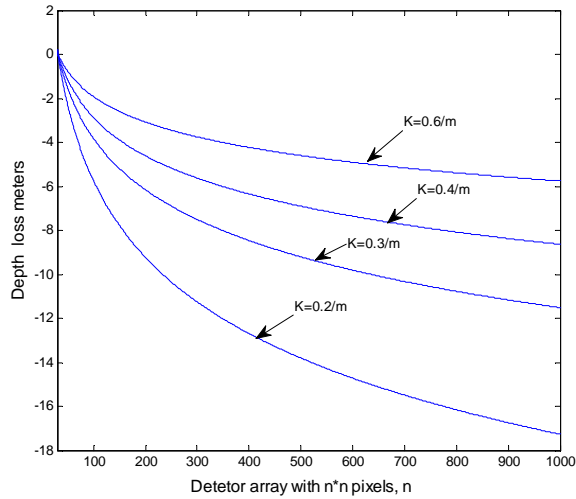


Figure 13. Estimated depth loss for an N*N gated imaging systems relative a conventional depth sounding single pixel lidar for different values of K.

8 Conclusions

For the first few metres below the sea surface, airborne and spaceborne passive multi- or hyperspectral imaging systems are of great interest for mapping as they offer increased possibilities to differentiate between habitat types. This is an important contribution in the near-shore and coastal zones. Passive sensors with high spatial resolution (metre-scale or better) are of largest interest for mapping, since the natural patchiness otherwise will blur the images and make classification less accurate. High spectral resolution or many "colour" bands in a passive sensor will result in better classification performance. Spectral reflectance data may additionally be used to monitor the health of the habitats. The required or optimal number of bands depends on which other data sources that are available, including their resolution. For example, Andrefouet *et al.* (Andrefouet *et al.* 2004) suggest that remote sensing with moderate spatial resolution (in their case CASI, 4 m pixels) can be used together with continuous spectral signatures acquired in situ at the centimetre scale to select key discrete wavelengths for remote-sensing observations of communities at the meter scale despite the spatial heterogeneity in benthic cover and the resulting spectral mixing.

For existing and new sensors, the methodology will be developed by better and more automated algorithms for data exploration and for fusing different data sets together. This includes both fusion of data from remote sensors (e.g. lidar and passive) and remote sensing data with in situ sampling. Also, fusion of remote sensing data e.g. with existing depth data digitised from hydrographic maps is a method that increase the value of passive remote sensing data compared to when it is used as single data source.

Airborne laser techniques for collection of depth can be considered as operational. Also, some promising pilot studies have been performed that have shown a potential to classify substrates and vegetation. With sensor and algorithm development the airborne depth sounding lidar is a highly interesting method for mapping of shallow underwater habitats. In general, the maximum depth range for airborne laser exceeds the possible depth range for passive sensors. Due to its high-resolution depth measurement capability, the lidar is able to capture different measures of bottom (or vegetation) roughness (rugosity, depth standard deviation, slopes etc), which have the potential to substantially improve classification and subsequent mapping of shallow benthic habitats.

Laser sensing will be further developed from line scanning and depth sounding lidars to include fluorescence, Raman and other spectral techniques to increase classification and concentration estimate of different objects and molecules. Laser imaging will be used taking advantage of high resolution 3D imaging as well as active multi- or hyperspectral capabilities. So far, classification of bottom vegetation using e.g. fluorescence, polarisation and Raman scattering has only been tested with special prototype systems from underwater platforms. Fluorescence has however several interesting features which might be useful in mapping of underwater habitats. One example is the laser induced fluorescence giving rise to the emission spectrum which could be used for classification together with e.g. the spectral reflectance signature. Another example is that in a time-resolved system, the fluorescence lifetime can indicate the health of plants. It should be noted that for underwater sensing the excitation wavelengths are limited to the visual region as e.g. ultraviolet radiation is highly attenuated in water. A problem with airborne fluorosensing of the sea floor is that the signal is much weaker than the elastically reflected signal. Future laser systems with higher efficiency together with high-sensitivity receivers may partly solve this problem. Another possibility are utilising fluorosensors mounted on underwater platforms operating a few metres above the bottom.

Recent development of broadband lasers and advanced imaging 3D receivers has led to new opportunities for advanced spectral and polarization imaging with high range resolution. The broad emission in supercontinuum white light lasers eliminates the problems with passive hyperspectral or multispectral imaging namely the conversion of the measured radiance to reflectance information. This conversion can be difficult for

passive sensors, due to the changing geometry between the sun, target and sensor which can affect the reflectance, and also introduce shadows in the scene. The inherent reflectance spectrum is one of the key measures for classification.

Platforms will continue to be developed for autonomous operation with the long term aim to reduce cost of operation and limit manpower involvement. Both underwater, surface and airborne platforms are included in this development. For example, there are several examples of existing airborne platforms with different size and payload capability. The smallest ones are cheap and can today carry passive camera equipment that may readily be useful for benthic habitat mapping in the most shallow areas.

References

- Airoidi, L. and Beck, M. W. 2007. Loss, status and trends for coastal marine habitats of Europe. In *Proceedings of Oceanography and Marine Biology: An Annual Review*, 2007, Taylor & Francis Vol. 45, 345-405.
- Andrefouet, S., Payri, C., Hochberg, E., Hu, C., Atkinson, M., and Muller-Karger, F. 2004. Use of in situ and airborne reflectance for scaling-up spectral discrimination of coral reef macroalgae from species to communities. *Marine ecology progress series* 283, 161-177.
- Barbini, R., Colao, F., Fantoni, R., Frassanito, C., Palucci, A., and Ribezzo, S. 2000. Range resolved lidar fluorosensor for marine investigation. In *Proceedings of EARSeL eProceedings*, Dresden, June 16-17 2000, EARSeL Vol. 175-184.
- Barbini, R., Colao, F., Fantoni, R., Fiorani, L., Okladnikov, I. G., and Palucci, A. 2005. Lidar calibrated satellite sensed primary production in the southern ocean. *Journal of Optoelectronics and Advanced Materials* 7, 1091-1101.
- Barbini, R., Colao, F., Fantoni, R., Fiorani, L., Kolodnikova, N. V., and Palucci, A. 2006. Laser remote sensing calibration of ocean color satellite data. *Annals of Geophysics* 49, 35-43.
- Barbini, R., Colao, F., Fantoni, R., Lazic, V., Palucci, A., Capitelli, F., and Steen, H. J. L. v. d. 2000. Laser induced breakdown spectroscopy for semi-quantitative elemental analysis in soils and marine sediments. In *Proceedings of EARSeL eProceedings*, Dresden, June 16-17 2000, EARSeL Vol. 122-129.
- Barth, H., Reuter, R., and Schröder, M. 2000. Measurement and simulation of substance specific contributions of phytoplankton, gelbstoff, and mineral particles to the underwater light field in coastal waters. In *Proceedings of EARSEL-SIG-Workshop LIDAR*, Dresden/FRG, 16-17 June 2000, EARSeL Vol. 165-174.
- Bensky, T. J., Clemo, L., Gilbert, C., Neff, B., Moline, M. A., and Rohan, D. 2008. Observation of nanosecond laser induced fluorescence of in vitro seawater phytoplankton. *Appl. Opt.* 47, 3980-3986.
- Bishop, G., Veiga, I. V., Watson, M., and Farr, L. 2007. Active spectral imaging for target detection. In *Proceedings of 4th EMRS DTC Technical Conference*, Edinburgh, 2007, Vol. B7.
- Brock, J. C., Wright, C. W., Kuffner, I. B., Hernandez, R., and Thompson, P. 2006. Airborne lidar sensing of massive stony coral colonies on patch reefs in the northern Florida reef tract. *Remote Sensing of Environment* 104, 31-42.
- Brown, C. E. and Fingas, M. F. 2003. Review of the development of laser fluorosensors for oil spill application. *Marine Pollution Bulletin* 47, 477-484.
- Busck, J. 2005. Underwater 3-D optical imaging with a gated viewing laser radar. *Opt. Eng.* 44, 116001-116001 - 116001-116007.
- Chekalyuk, A. M., Hoge, F. E., Swift, R. N., and Yungel, J. K. 2003. New technological developments for ocean LIDAR biomonitoring. In *Proceedings of Ocean Remote Sensing and Imaging II*, 2003, SPIE Vol. 5155,
- Churnside, J. H. and Wilson, J. J. 2001. Airborne lidar for fisheries applications. *Opt. Eng.* 40, 406-414.
- Churnside, J. H. and Wilson, J. J. 2004. Airborne lidar imaging of salmon. *Applied Optics* 43, 1416-1424.
- Churnside, J. H., Wilson, J. J., and Tatarskii, V. V. 1997. Lidar profiles of fish schools. *Appl. Opt.* 36, 6011-6020.

- Chust, G., Galparsoro, I., Borja, A., Franco, J., and Uriarte, A. 2008. Coastal and estuarine habitat mapping, using LIDAR height and intensity and multi-spectral imagery. *Estuarine, Coastal and Shelf Science* 78, 633-643.
- Clemenceau, P., Dogariu, A., and Stryewski, J. 2000. Polarization active imaging. In *Proceedings of Laser Radar Technology and Applications V*, 2000, SPIE Vol. 4035, 401-409.
- Coggan, R., Populus, J., J., W., Sheehan, K., F., F., and Pile, S. 2007. (eds.) Review of standards and protocols for seabed habitat mapping. MESH [www. searchmesh.net/](http://www.searchmesh.net/), 1-203.
- Collin, A., Archambault, P., and Long, B. 2008. Mapping the shallow water seabed habitat with the SHOALS. *IEEE Transactions on Geoscience and Remote Sensing* 46.
- Costa, B. M., Battista, T. A., and Pittman, S. J. 2009. Comparative evaluation of airborne LiDAR and ship-based multibeam SONAR bathymetry and intensity for mapping coral reef ecosystems. *Remote Sensing of Environment* 113, 1082-1100.
- DeWeert, M. J., Moran, S. E., Ulich, B. L., and Norris, R. N. 1999. Numerical simulations of the relative performance of streak-tube, range-gated, and PMT-based airborne imaging lidar systems with realistic sea surfaces. In *Proceedings of Airborne and In-Water Underwater Imaging*, Denver, Colorado, July 1999, SPIE Vol. 3761, 115-129.
- Fantoni, R., Barbini, R., Colao, F., Ferrante, D., Fiorani, L., and Palucci, A. 2004. Integration of two lidar fluorosensor payloads in submarine ROV and flying UAV platforms. In *Proceedings of EARSeL eProceedings*, 2004, EARSeL Vol. 3, 1/2004, 43-53.
- Fefilatyeve, S., Goldgof, D. B., and Lembke, C. 2009. Autonomous buoy platform for low-cost visual maritime surveillance: design and initial deployment. In *Proceedings of Ocean Sensing and Monitoring*, 2009, SPIE Vol. 7317, 73170A-73171 -- 73112.
- Feigels, V. I. and Kopilevich, Y. I. 1999. Russian airborne lidar systems: comparative analysis and new ideas. In *Proceedings of Conference on Airborne and In-Water Underwater Imaging*, Denver, Colorado, July 1999, SPIE Vol. 3761, 130-141.
- Feygels, V. I., Kopilevich, Y. I., Surkov, A., Yungela, J. K., and Behrenfeld, M. J. 2005. Airborne lidar system with variable field-of-view receiver for water optical properties measurement. In *Proceedings of Ocean Remote Sensing and Imaging II*, 2005, SPIE Vol. 5155, 12-21.
- Foster, J., Riegl, B., Purkis, S., and Dodge, R. 2006. Mapping of Tropical Shallow Water Benthos (Algae, Seagrass, Corals) Using Three Single-Beam Acoustic Ground Discrimination Systems (QTCView, Echoplus, Biosonics). *EOS, Transactions, American Geophysical Union* 87.
- Foster, R. and Jesus, B. 2006. Field spectroscopy of estuarine intertidal habitats. *International Journal of Remote Sensing* 27, 3657-3669.
- Fournier, G. R., Bonnier, D., Forand, J. L., and Pace, P. W. 1993. Range-gated underwater laser imaging system. *Opt. Eng.* 32, 2185-2190.
- Garcia, C. S., Abedin, M. N., Ismail, S., Sharma, S. K., Misra, A. K., Nguyen, T., and Elsayed-Ali, H. 2009. Studies of minerals, organic and biogenic materials through time-resolved Raman spectroscopy. In *Proceedings of Advanced Environmental, Chemical, and Biological Sensing Technologies VI*, 2009, SPIE Vol. 7312, 731210-731211 -- 731219.
- Gibbs, A. E., Cochran, S. A., Logan, J. B., and Grossman, E. E. 2006. *Benthic habitats and offshore geological resources of Kaloko-Honokōhau national historical park, Hawaii*. Scientific Investigations Report 2006-5256. U.S. Dept of Interior, U.S. Geological Survey. .
- Gleckler, A. D., Gelbart, A., and Bowden, J. M. 2001. Multispectral and hyperspectral 3D imaging lidar based upon the multiple slit streak tube imaging lidar. In *Proceedings of Laser Radar and Technology Applications VI*, 2001, SPIE Vol. 4377, 328-335.
- Goda, K., Tsia, K. K., and Jalali, B. 2009. Serial time-encoded amplified imaging for real-time observation of fast dynamic phenomena. *Nature*.

- Harsdorf, S., Janssen, M., Reuter, R., Toeneboen, S., Wachowicz, B., and Willkomm, R. 1999. Submarine lidar for seafloor inspection. *Meas. Sci. Technol.* 10, 1178-1184.
- Hilldale, R. C. and Raff, D. 2007. Assessing the ability of airborne LiDAR to map river bathymetry. *Earth Surface Processes and Landforms* 33, 773-783.
- Hochberg, E. J. and Atkinson, M. J. 2008. Coral reef benthic productivity based on optical absorptance and light-use efficiency. *Coral Reefs* 27, 49-59.
- Hou, W. and Weidemann, A. D. 2009. Diver visibility: why one can not see as far? In *Proceedings of Ocean Sensing and Monitoring*, 2009, SPIE Vol. 7317, 73170I-73171 -- 73177.
- The Infrared & Electro-Optical Systems Handbook*. 1993. Vol. 6. Bellingham: SPIE Optical Engineering Press.
- Isaeus, M. 2004. Factors structuring Fucus communities at open and complex coastlines in the Baltic Sea. Ph D Thesis thesis, Department of Botany, Stockholm University, Stockholm, Sweden.
- Jaffe, J. S., McLean, J., Strand, M. P., and Moore, K. D. 2001. Underwater optical imaging: status and prospects. *Oceanography* 13, 66-76.
- Karpicz, R., Dementjev, A., Kuprionis, Z., Pakalnis, S., Westphal, R., Reuter, R., and Gulbinas, V. 2006. Oil spill fluorosensing lidar for inclined onshore or shipboard operation. *Appl. Opt.* 45, 6620-6625.
- Kautsky, H. 2009. Guidelines for the Sampling of Marine Phytobenthic Communities. *ICES Techniques in Marine Environmental Sciences No. 44, June 2009 (in print)*.
- Kopilevich, Y. I., Feygels, V. I., Tuell, G. H., and Surkov, A. 2005. Measurement of ocean water optical properties and seafloor reflectance with Scanning Hydrographic Operational Airborne Lidar Survey (SHOALS): I. Theoretical background. In *Proceedings of Remote Sensing of the Coastal Oceanic Environment*, 2005, SPIE Vol. 5885, 58850D-58851 -- 58859.
- Kratzer, S. and Tett, P. 2009. Using bio-optics to investigate the extent of coastal waters: A Swedish case study. *Hydrobiologia* 629, 169-186.
- Kuffner, I. B., Brock, J. C., Grober-Dunsmore, R., Bonito, V. E., Donald, H. T., and Wayne, W. C. 2007. Relationships between reef fish communities and remotely sensed rugosity measurements in Biscayne National Park, Florida, USA. *Environmental Biology of Fishes* 78, 71-82.
- Kutser, T., Dekker, A. G., and Skirving, W. 2003. Modeling spectral discrimination of Great Barrier Reef benthic communities by remote sensing instruments. *Limnology and Oceanography* 48, 497-510.
- Kutser, T., Vahtmae, E., and Martin, G. 2006. Assessing suitability of multispectral satellites for mapping benthic macroalgal cover in turbid coastal waters by means of model simulations. *Estuarine, Coastal and Shelf Science* 67, 521-529.
- Kutser, T., Vahtmäe, E., and Metsamaa, L. 2006. Spectral library of macro algae and benthic substrates in Estonian coastal waters. *Proceedings of Estonian Academy of Science* 55, 329-340.
- Kutser, T., Vahtmae, E., and Metsamaa, L. 2006. Spectral library of macroalgae and benthic substrates in Estonian coastal waters. In *Proceedings of Estonian Acad. Sci. Biol. Ecol.*, 2006, Vol. 55, 329-340.
- Lee, Z., Carder, K. L., Mobley, C. D., Steward, R. G., and Patch, J. S. 1998. Hyperspectral remote sensing for shallow waters: 1. A semianalytical model. *Applied Optics* 37, 6329-6338.
- Lee, Z., Carder, K. L., Mobley, C. D., Steward, R. G., and Patch, J. S. 1999. Hyperspectral remote sensing for shallow waters: 2. Deriving bottom depths and water properties by optimization. *Applied Optics* 38, 3831-3843.

- Lee, Z., Carder, K. L., Hawes, S. K., Steward, R. G., Peacock, T. G., and Davis, C. O. 1994. Model for the interpretation of hyperspectral remote-sensing reflectance. *Appl. Opt.* 33, 5721-5732.
- Malthus, T. J. and Karpouzli, E. 2003. Integrating field and high spatial resolution satellite-based methods for monitoring shallow submersed aquatic habitats in the Sound of Eriskay, Scotland, UK. *Int. J. Remote Sensing* 24, 2585-2593.
- Maritorea, S., Morel, A., and Gentili, B. 1994. Diffuse Reflectance of Oceanic Shallow Waters : Influence of the Water Depth and Bottom Albedo. *Limnology and Oceanography* 39, 1689.
- Maslov, D. V., Fadeev, V. V., and Lyashenko, A. I. 2000. A shore-based lidar for coastal seawater monitoring. In *Proceedings of EARSeL eProceedings*, Dresden, June 16-17 2000, EARSeL Vol. 46-52.
- Measures, R. M. 1984. *Laser remote sensing - fundamentals and applications*. 1992 ed. New York: Wiley and Sons.
- Méléder, V., Populus, J., and Rollet, C. 2007. *Mapping seabed substrata using Lidar remote sensing*. Action 4. MESH. <http://www.searchmesh.org/default.aspx>
- Mishra, D., R., Narumalani, S., Rundquist, D., Lawson, M., and Perk, R. 2007. Enhancing the detection and classification of coral reef and associated benthic habitats: A hyperspectral remote sensing approach. *Journal of Geophysical Research. C. Oceans* 112.
- Mobley, C. D. 1994. *Light and Water*. San Diego: Academic Press.
- Mochi, I., Bazzani, M., Cecchi, G., Cucci, C., Lognoli, D., Pantani, L., Raimondi, V., Tirelli, D., Valmori, G., Abbate, M., and Fontani, S. 2002. High-resolution lidar fluorescence spectra for the characterization of phytoplankton. In *Proceedings of Remote Sensing of the Ocean and Sea Ice 2002*, 2002, SPIE Vol. 4880, 117-126.
- Moore, K. D., Jaffe, J. S., and Ochoa, B. L. 2000. Development of a new underwater bathymetric laser imaging system: L-Bath. *Journal of Atmospheric and Oceanic Technology* 17, 1106-1117.
- Moran, S., Austin, W., Murray, J., Roddier, N., Bridges, R., Vercillo, R., Stettner, R., Phillips, D., Bisbee, A., and Witherspoon, N. 2003. Rapid overt airborne reconnaissance (ROAR) for mines and obstacles in very shallow water, surf zone, and beach. In *Proceedings of Detection and Remediation Technologies for Mines and Minelike Targets VIII*, 2003, SPIE Vol. 5089, 214-224.
- Morvan, L., Alouini, M., Grisard, A., Lallier, E., and Dolfi, D. 2004. Two optronic identification techniques: lidar-radar and multispectral polarimetric imaging. In *Proceedings of Military Remote Sensing*, 2004, SPIE Vol. 5613, 76-87.
- Mumby, P. J., Clark, C. D., Green, E. P., and Edwards, A. J. 1998. Benefits of water column correction and contextual editing for mapping coral reefs. *International Journal of Remote Sensing* 18, 203-210.
- Nassef, O. A. and Elsayed-Ali, H. E. 2009. Absorption laser-induced breakdown spectroscopy. In *Proceedings of Advanced Environmental, Chemical, and Biological Sensing Technologies VI*, 2009, SPIE Vol. 7312, 73120Z-73121 -- 73127.
- Naturvårdsverket. 2008. *Utbredning av arter och naturtyper på utsjögrund i Östersjön, en modelleringsstudie*. Naturvårdsverket Rapport 5817. Stockholm:
- Naturvårdsverket. 2009. *Naturtyper på havets botten baserat på art- och habitat modellering*. Naturvårdsverket Rapport 5987. Stockholm:
- Nayegandhi, A., Brock, J. C., and Wright, C. W. 2009. Small-footprint, waveform-resolving lidar estimation of submerged and sub-canopy topography in coastal environments . . . *International Journal of Remote Sensing* 30, 861-878.

- Nischan, M. L., Joseph, R. M., Libby, J. C., and Kerekes, J. P. 2003. Active Spectral Imaging. *Lincoln Laboratory Journal* 14, 131-144.
- Pe'Eri, S., Gardner, J. V., Ward, L. G., Morrison, R. J., and Lillycrop, J. 2007. Identifying Subtidal Coastal Environments Using Airborne Lidar Bathymetry (ALB) *American Geophysical Union, Fall Meeting 2007, abstract #H51L-07*.
- Phinn, S., Roelfsema, C., Dekker, A., Brando, V., and Anstee, J. 2008. Mapping seagrass species, cover and biomass in shallow waters: An assessment of satellite and airborne multispectral and airborne hyper-spectral imaging systems in Moreton Bay (Australia). *Remote Sensing of Environment* 112, 3413-3425.
- Populus, J., Laurentin, A., Rollet, C., Vasquez, M., Guillaumont, B., and Bonnot-Courtois, C. 2004. Surveying coastal zone topography with airborne remote sensing for benthos mapping. In *Proceedings of EARSeL eProceedings*, 2004, EARSeL Vol. 3, 1/2004, 105-117.
- Poryvkina, L., Babichenko, S., and Leeben, A. 2000. Analysis of phytoplankton pigments by excitation spectra of fluorescence. In *Proceedings of EARSEL-SIG-Workshop LIDAR*, Dresden/FRG, 16-17 June 2000, EARSeL Vol. 224-232.
- Precision-Identification. 2002. *Eelgrass Mapping Review*. Vancouver, B.C.: Precision Identification.
- Rhoads, D. C. and Germano, J. D. 1982. Characterization of benthic processes using sediment-profile imaging: an efficient method of Remote Ecological Monitoring Of The Seafloor *Marine ecology progress series* 8, 115-128.
- Sabins, F. F. 1997. *Remote sensing: Principles and Interpretation*. 3rd ed. New York: Freeman.
- Sabol, B., Lord, E., Reine, K., and Shafer, D. 2008. *Comparison of acoustic and aerial photographic methods for quantifying the distribution of submersed aquatic vegetation in Sagamore Creek, NH* DOER-E23. Vicksburg, MS: U.S. Army Engineer Research and Development Center.
- Samson, G., Tremblay, N., Dudelzak, A. E., Babichenko, S. M., Dextraze, L., and Wollring, J. 2000. Nutrient stress of corn plants: Early detection and discrimination using a compact multiwavelength fluorescent lidar. In *Proceedings of EARSeL eProceedings*, Dresden, June 16-17 2000, EARSeL Vol. 214-223.
- Schofield, O., Kohut, J., and Glenn, S. 2009. Using Webb gliders to maintain a sustained ocean presence. In *Proceedings of Ocean Sensing and Monitoring*, 2009, SPIE Vol. 7317, 731707-731701 -- 731707.
- Shumway, C. A., Hofmann, H. A., and Dobberfuhl, A. P. 2007. Quantifying habitat complexity in aquatic ecosystems *Freshwater Biology* 52, 1065-1076.
- Steinval, O., Andersson, P., Elmqvist, M., and Tulldahl, H. M. 2007. Overview of range gated imaging at FOI. In *Proceedings of Infrared Technology and Applications XXXIII*, 2007, SPIE Vol. 6542, 654216-654211 -- 654213.
- Stumpf, R. P., Holderied, K., and Sinclair, M. 2003. Determination of water depth with high-resolution satellite imagery over variable bottom types. *Limnol. Oceanogr.* 48, 547-556.
- Stute, U., Haître, M. L., and Lado-Bordowsky, O. 2002. Temporal aspects of fluorescence - in-situ analysis with a bistatic submarine Lidar. In *Proceedings of Atmospheric and Ocean Optics*, 2002, SPIE Vol. 4678, 289-300.
- Therriault, C., Hatcher, B. G., Scheibling, R. E., and Jones, W. 2006. Mapping the Distribution of an Invasive Marine Alga (*Codium fragile*) in Optically Shallow Coastal Waters Using the Compact Airborne Spectrographic Imager (casi). *EOS, Transactions, American Geophysical Union* 87.

- Thorhaug, A., Richardsson, A. D., and Berlyn, G. P. 2007. Spectral reflectance of the seagrasses: *Thalassia testudinum*, *Halodule wrightii*, *Syringodium filiforme* and five marine algae. *Int. J. Remote Sensing* 28, 1487-1501.
- Tuell, G. and Park, J. Y. 2004. Use of SHOALS bottom reflectance images to constrain the inversion of a hyperspectral radiative transfer model. In *Proceedings of Laser Radar and Technology Applications IX*, Orlando, FL, 12–16 April 2004, SPIE Vol. 5412, 185-193.
- Tuell, G., Park, J. Y., Aitken, J., Ramnath, V., Feygels, V., Guenther, G., and Kopilevich, Y. 2005. SHOALS-enabled 3-d benthic mapping. In *Proceedings of Algorithms and Technologies for Multispectral, Hyperspectral, and Ultraspectral Imagery XI*, Orlando, FL, 28 March–1 April 2005, SPIE Vol. 5806, 816-826.
- Tulldahl, H. M. and Wikström, S. A. 2010. *Initial report on statistical separability of vegetation and bottom types in laser data*. FOI-R--2961--SE. Linköping, Sweden: Swedish Defence Research Agency.
- Tulldahl, H. M. and Pettersson, M. 2007. Lidar for shallow underwater target detection. In *Proceedings of Electro-Optical Remote Sensing, Detection, and Photonic Technologies and their Applications*, Florence, Italy, 17-20 September 2007, SPIE Vol. 6739, 673906-673901 -- 673912.
- Tulldahl, H. M., Vahlberg, C., Axelsson, A., and Janeke, H. 2008. Sea floor characterization from airborne lidar data. In *Proceedings of International Lidar Mapping Forum 08*, Denver, USA, Februari 21-22 2008, Vol.
- Tulldahl, H. M., Andersson, P., Olsson, A., and Andersson, A. 2006. Experimental evaluation of underwater range-gated viewing in natural waters. In *Proceedings of Electro-Optical and Infrared Systems: Technology and Applications III*, Stockholm, Sweden, 13-14 September 2006, SPIE Vol. 6395, 639506-639501 - 639506-639508.
- Tulldahl, H. M., Vahlberg, C., Axelsson, A., Karlsson, H., and Jonsson, P. 2007. Sea floor classification from airborne lidar data. In *Proceedings of Lidar Technologies, Techniques, and Measurements for Atmospheric Remote Sensing III*, Florence, Italy, 17-20 September 2007, SPIE Vol. 6750, 675003-675001 -- 675012.
- Ulich, B. L., Lacovara, P., Moran, S. E., and Deweert, M. J. 1997. Recent results in imaging lidar. In *Proceedings of Advances in Laser Remote Sensing for Terrestrial and Hydrographic Applications*, April 1997, SPIE Vol. 3059,
- Waddington, T. and Hart, K. 2003. *Tools and Techniques for the Acquisition of Estuarine Habitat Data - Final Report*. SAIC Report No. 628. Charleston, SC: NOAA Coastal Services Center.
- Vahtmäe, E. and Kutser, T. 2007. Mapping of bottom type and water depth in shallow coastal waters with satellite remote sensing. *Journal of Coastal Research*, 185-189.
- Wedding, L., M., Friedlander, A. M., McGranaghan, M., Yost, R., S., and E., M. M. 2008. Using bathymetric LIDAR to define nearshore benthic habitat complexity: Implications for management of reef fish assemblages in Hawaii . . *Remote Sensing of Environment* 112, 4159-4165.
- Wennberg, S., Evertson, J., Bergström, U., Sundblad, G., Sandström, A., and Karås, P. 2007. *Evaluation of satellite imagery as a tool to characterise shallow habitats in the Baltic Sea*. Stockholm, Sweden: Metria Miljöanalys.
- Zhou, J., Tonizzo, A., Gilerson, A., Twardowski, M., Gray, D., Weidemann, A., Arnone, R., Gross, B., Moshary, F., and Ahmed, S. 2009. Polarization characteristics of coastal waters and their impact on in-water visibility. In *Proceedings of Ocean Sensing and Monitoring*, 2009, SPIE Vol. 7317, 73170H-73171 -- 73178.
- Zielinski, O., Andrews, R., Göbel, J., Hanslik, M., Hunsänger, T., and Reuter, R. 2000. operational airborne hydrographic laser fluorosensing. In *Proceedings of EARSEL-SIG-Workshop LIDAR*, Dresden/FRG, 16-17 June 2000, EARSeL Vol. 53-60.